TÉCNICO LISBOA

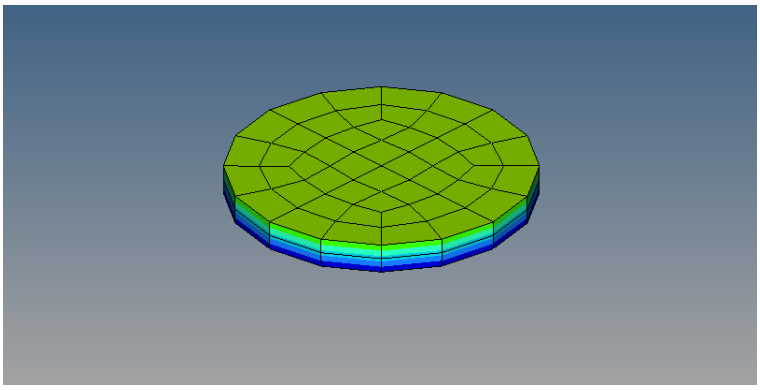

Mechanical behaviour of complex structures under high speed impacts

Bruno Aires de Albuquerque e Concha de Almeida

Thesis to obtain the Master of Science Degree in

Aerospace Engineering

Supervisor(s): Luís Filipe Galrão dos Reis, PhD, IST-UL
Pedro Miguel de Almeida Talaia, PhD, CEIIA

Examination Committee

Chairperson: Filipe Szolnoky Ramos Pinto Cunha, PhD, IST-UL
Supervisor: Luís Filipe Galrão dos Reis, PhD, IST-UL
Member of the Committee: Miguel António Lopes de Matos Neves, PhD, IST-UL

November 2016

Dedicated to my grandfather

Acknowledgments

First of all I would like to thank my girlfriend Rita Nascimento for all the patience, motivation and happiness during the last years and in particular this last one. Also to her parents Adelaide and Manuel for all the support during the degree as they were nothing more than parents to me. Beyond, David Brandão and José Fernandes for all the late night studying and for all the amazing years in the university, for all the happy moments and for the ones that will come for sure. To my family I must thank for making me who I am and for helping and motivating me to enter the degree I have always wanted. A special thanks to my best friend Tiago Fachada can not be forgot once he was the basis of some good and necessary distractions, good laughs and night walks over the time we met.

Finally I can not forget my two supervisors Prof. Luís Reis and Dr. Pedro Talaia for the patience in guiding me through this thesis and readiness in help and also CEIIA for the opportunity of developing this master thesis in a modern business environment.

Resumo

De acordo com as mais recentes necessidades globais, o uso de materiais renováveis, com produção não poluente e baratos têm vindo a ser recorrentemente incorporados em variados componentes de indústrias como a aeronáutica, a automóvel e mesmo a de segurança. Neste sentido a cortiça surge como um material celular natural com boas características no campo da absorção de energia, de peso e mesmo da possibilidade de ser colocada sob impactos múltiplos e ainda assim manter as suas boas características. No entanto, este material possui um comportamento bastante diferente dos materiais habituais devido quer ao seu comportamento mecânico quer à sua variabilidade e como tal a sua caracterização torna-se difícil. De forma a tentar responder a este problema recorreu-se a um algoritmo explícito de elementos finitos, LS-DYNA, e às cartas de modelos de materiais que este possui de forma a aproximar, com os dados existentes, o comportamento da cortiça aglomerada ao comportamento de uma espuma convencional de baixa densidade ou de um honeycomb. Esta caracterização, cujo procedimento se encontra descrito nesta tese, pretende proceder à caracterização da cortiça sujeita a compressão a diferentes taxas de deformação e desta forma completar parte de um modelo que possa representar o aglomerado de cortiça, NL20, o mais exatamente possível em qualquer tipo de esforço. Após concluída a modelação procede-se à aplicação deste modelo a 3 casos de estudo em que este material é usado em componentes onde faça sentido a utilização das características da cortiça podendo-se por fim concluir sobre a possibilidade de integração desta em diferentes ambientes.

Palavras-chave: Cortiça, Aglomerado de Cortiça, NL20 , Algoritmo Explícito, Elementos Finitos, LS-DYNA, Absorção de Energia

Abstract

In accordance with the actual global necessities, the use of renewable materials, with non pollutant production and cheap are being incorporated in various components in various industries as for example the aeronautical, automotive and even security. In this way, agglomerated cork presents itself as a natural cellular material with good characteristics of energy absorption, weight and the possibility of being used under multiple impacts and still maintain its characteristics. However this material has a behaviour much different from the usual because of its mechanical behaviour and variability, which makes its characterization difficult. As a way to try to solve this problem, one recurred to an explicit algorithm of finite elements, LS-DYNA, and its cards of material models to try to approximate, with the available data, the behaviour of agglomerated cork, NL20, to the behaviour of a standard foam or a honeycomb. This procedure, described in this thesis, aims to characterize the agglomerated cork's behaviour in compression in different strain rates and by this means to complete part of a model that would describe as good as possible the agglomerated behaviour under this kind of effort. Done this, the model is applied to 3 case studies where agglomerated cork is used in components where it makes sense and where its characteristics may be advantageous so that in the end one can conclude about the possibility of integrating this material in different environments.

Keywords: Cork, Agglomerated Cork, NL20, Explicit Algorithms, Finite Elements , LS-DYNA, Energy Absorption

Contents

Acknowledgments v
Resumo vii
Abstract ix
List of Tables xiii
List of Figures xv
Nomenclature xvii
Glossary xxiii

1 Introduction **1**
1.1 Motivation 2
1.2 Topic Overview 2
1.3 Objectives 6
1.4 Thesis Outline 6

2 Background **9**
2.1 Theoretical Overview 9
2.1.1 Cellular Materials 9
2.2 LS-DYNA Model 1- Honeycomb 15
2.3 LS-DYNA Model 2-Low Density Foam 17

3 Implementation **21**
3.1 Numerical Model 22
3.1.1 Mesh 22
3.1.2 Models Inputs 23
3.2 Experimental Results 25

4 Results **27**
4.1 Honeycomb Results 27
4.1.1 Solid Formulation 1 27
4.1.2 Solid Formulation -1 29
4.2 Low Density Foam Results 30
4.2.1 Solid Formulation 1 30

4.2.2 Solid Formulation 2 32
4.2.3 Solid Formulation 3 33
4.2.4 Solid Formulation -1 34
4.2.5 Solid Formulation -2 35
4.3 Model Selection 37
4.4 Model update for strain rate effects 38
4.5 Case Study 1 - 3 Point Bending 41
4.6 Case Study 2 - Jet Engine Blade Containment 45
4.7 Case Study 3 - Ballistic Impact on sandwich panel 47

5 Conclusions and Future Work **51**
5.1 Conclusions 51
5.2 Future Work 52

Bibliography **53**

A Cork **57**
A.0.1 Cork 57

B Finite Element Method-LS-DYNA **63**
B.0.1 Finite Element Method 63
B.0.2 Optimization Technique 68

List of Tables

3.1 Honeycomb model inputs 23
3.2 Low density foam model inputs 24

4.1 Simulation Information of Honeycomb form.1 28
4.2 Simulation Information of Honeycomb form.-1 30
4.3 Simulation Information of LDF form.1 31
4.4 Simulation Information of LDF form.2 33
4.5 Simulation Information of LDF form.3 34
4.6 Simulation Information of LDF form.-1 35
4.7 Simulation Information of LDF form.-2 36
4.8 Tune for 500 s^{-1} 39
4.9 Tune for 1000 s^{-1} 40
4.10 Specimen Data 41
4.11 Simulation Results 46
4.12 Kinetic Energy Data 48
4.13 Kinetic Energy data for 10mm cork core 49
4.14 Kinetic Energy data for 40mm cork core 50

List of Figures

1.1 Cellular Materials Multi Functionality. 1

2.1 Artificial cellular Materials 10
2.2 Natural cellular Materials 10
2.3 Cell. 11
2.4 Cellular Materials Behaviour 11
2.5 Energy Absorption plot. 14

3.1 Schematics of the compression test and specimen used. 21
3.2 Rough meshes 22
3.3 Refined meshes 23
3.4 Stress vs Strain NL10 and NL20 24
3.5 NL20 Behaviour (Prof. Pedro Rosa to Amorim Composites report). 25

4.1 Honeycomb Formulation 1 Results 28
4.2 Energies vs Time of Honeycomb model form.1 28
4.3 Honeycomb Formulation -1 Results 29
4.4 Energies vs Time of Honeycomb model form.-1 30
4.5 Low density foam Formulation 1 Results 31
4.6 Energies vs Time of LDF model form.1 31
4.7 Low density foam Formulation 2 Results 32
4.8 Energies vs Time of LDF model form.2 32
4.9 Low density foam Formulation 3 Results 33
4.10 Energies vs Time of LDF model form.3 34
4.11 Low density foam Formulation -1 Results 34
4.12 Energies vs Time of LDF model form.-1 35
4.13 Low density foam Formulation -2 Results 36
4.14 Energies vs Time of LDF model form.-2 36
4.15 Models errors and Standard Deviation in Elastic Region 37
4.16 Models errors and Standard Deviation in the Plateau Region 37
4.17 Models errors and Standard Deviation in the Densification Region 38
4.18 Strain Rate 500 s^{-1} behaviour 39

4.19 Strain Rate 1000 s^{-1} behaviour . . . 40
4.20 Strain Rate sensibility . . . 41
4.21 Setup . . . 42
4.22 Bending Results . . . 42
4.23 Bending results for formulation -1 . . . 43
4.24 Bending results scaled . . . 44
4.25 Bending results for changed Young Modulus . . . 44
4.26 Von Mises bending results . . . 45
4.27 Results without cork . . . 46
4.28 Results with cork . . . 46
4.29 Mesh and setup to ballistic impact test . . . 47
4.30 Von Mises Stresses in Ballistic Impact . . . 47
4.31 Ballistic Impact at 200m/s on 10mm core sandwich . . . 48
4.32 Ballistic Impact at 400m/s on 10mm core sandwich . . . 48
4.33 Ballistic Impact at 1000m/s on 10mm core sandwich . . . 48
4.34 Ballistic Impact at 200 m /s on 40mm core sandwich . . . 49
4.35 Ballistic Impact at 400 m /s on 40mm core sandwich . . . 49
4.36 Ballistic Impact at 1000 m /s on 40mm core sandwich . . . 49
4.37 Absorbed Energy vs Impact K . . . 50

A.1 Cork. . . . 57
A.2 Process of cork harvesting. . . . 58
A.3 Hooke cork observation. . . . 59
A.4 Cork main directions. . . . 59
A.5 Cork Cell. . . . 60
A.6 Cork mechanical behaviour . . . 60

B.1 Body and Notation . . . 63
B.2 Formulation 1 . . . 65
B.3 Formulation 2 . . . 66
B.4 Formulation -1 . . . 66
B.5 Formulation -2 . . . 66
B.6 Formulation 3 . . . 67
B.7 Hourglass modes. . . . 67

.

Nomenclature

Greek symbols

ϖ	Traction Tensor.
Δ	Variation.
δ	Kronecker delta.
ϵ	Strain.
η	Nominal Stresses.
λ	Stretches.
ω_1	Factor associated with the constrains in the body.
ω_2	Factor associated with the constrains in the body.
ϕ	Volume fraction of solid in cell edges.
ρ	Density.
σ	Stress.
τ	Time.
θ	Angle between the biggest and smallest cell's side.
υ	Poisson Coefficient.
ξ, η, ζ	Parametric coordinates.

Roman symbols

$[B]$	Strain Displacement matrix.
$\boldsymbol{F}$	Stress divergence vector.
$\ddot{x}_i$	Acceleration at a given instant.
$\dot{x}_i$	Velocity at a given instant.
a	Acceleration vector.

b	Cell height.
c	Adiabatic sound velocity.
d	Displacement.
E	Young Modulus.
e	Napier's Constant.
f	Body forces.
G	Shear Modulus.
H	Hourglass resistance effect.
h	Biggest cell's side length.
I	Inertia Moment associated with the solid section.
K	Bulk Modulus.
k	Node number
L	Specimen Length.
l	Smallest cell's side length.
M	Mass.
N	Shape Function
P	Load.
p	Pressure.
Q	Value given in function of the bulk viscosity.
q	Bulk viscosity.
S	Surface Area.
s	Stress.
t	Cell's wall thickness.
V	Volume.
v	Velocity.
W	Energy absorbed during deformation.
x	Position.
EAAU	Elastic modulus Eaau in uncompressed configuration.

EBBU Elastic modulus Ebbu in uncompressed configuration.

ECCU Elastic modulus Eccu in uncompressed configuration.

GABU Shear modulus Gabu in uncompressed configuration.

GBCU Shear modulus Gbcu in uncompressed configuration.

GCAU Shear modulus Gcau in uncompressed configuration.

LCA Load curve for σ-aa versus either relative volume or volumetric strain

LCAB Load curve for σ-ab versus either relative volume or volumetric strain.

LCB Load curve for σ-bb versus either relative volume or volumetric strain.

LCBC Load curve for σ-bc versus either relative volume or volumetric strain.

LCC Load curve for σ-cc versus either relative volume or volumetric strain.

LCCA Load curve for σ-ca versus either relative volume or volumetric strain.

LCID Load curve or table for the nominal stress versus strain curve definition;

LCS Load curve for shear stress versus either relative volume or volumetric strain.

LCSR Load curve for strain-rate effects defining the scale factor versus strain rate.

SSEF Shear strain at element failure (element will erode).

TSEF Tensile strain at element failure (element will erode).

Subscripts

0 Initial.

$1, 2, 3$ Cartesian components.

a, b, c Cartesian components.

atm Atmospheric.

cr Critical.

D Densification region.

el Elastic Stress.

fc Fully compressed.

fs Face Stretching.

i, j, k Cartesian components.

max Maximum value.

p Peak.

r Relative.

s Solid material component.

T Total.

u Uncompressed Configuration.

ys Yield Stress.

Superscripts

$*$ Cellular material component.

. First time derivative.

.. Second time derivative.

dev Deviatronic.

f Foam Component.

n Time step.

r Rate Effects.

T Transpose

Glossary

CFRP Carbon Fiber Reinforced Plastic is a composite material constituted by a thermosetting resin and carbon fibers to add strength.

CPU Central Processing Unit.

EPS Expanded Polystyrene is a foam that can be used in many industries from technology to design and even food.

FEA Finite Element Analysis is the application of a numerical tool to find approximate solutions to differential equations.

FEM Finite Element Method is the methodology/algorithms used in FEA.

Form Solid Formulation.

LDF Low Density Foam.

PVC Polyvinyl chloride is used as rigid or flexible and can be applied in pipes, profiles, cards, electrical cable insulation or even leather imitation.

Chapter 1

Introduction

Nowadays sandwich panels are used in many applications for their advantageous characteristics of specific rigidity, weight, bending, impact and additionally perform very well as acoustical and thermal insulator assuming a position of multi-functional material. On the other hand some structural problems may arise due to the combination of a soft core with rigid sheets that are usually made of a different material and even problems related to the recycling of this material which is getting more important everyday.
There are many materials that can constitute the core of the sandwich material, one of the most important kind are the cellular ones that can be used in a variety of applications as can be seen in following figure 1.1.

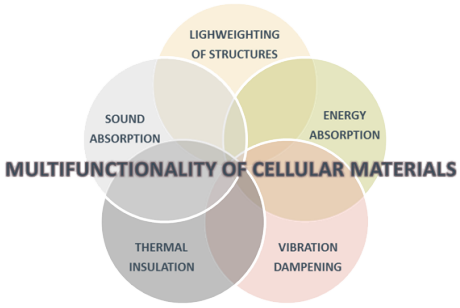

Figure 1.1: Cellular Materials Multi Functionality (Source [1])

In the energy absorption field, one important application for cellular materials such as metal and polymeric foams is impact. Due to the material nature, these materials can absorb a huge quantity of energy and be lightweight at the same time. However when the impact is due to a projectile these materials need to be associated with other materials better to withstand the projectile impact.
With everything in mind, this document can provide guidelines to this kind of study and specifically to cellular materials, making the process faster and more accurate letting engineers with more time to optimization processes. Trying to give one step forward in the cellular materials theme, this master thesis intends to increase the knowledge in this area and apply it to composites sandwich materials

once their use can be beneficial in various fields from aeronautics, automotive and personal security to military and police forces.

1.1 Motivation

For many years designing with basis on functionality was the main aim of engineers. However, nowadays new challenges are presented and the idea above is not sufficient any more. With the new challenges in mind, engineers need to design based not only on functionality but also need to predict life and structural response under abnormal circumstances. In engineering, composites are being used increasingly in many areas, the main advantage of this kind of material is that by joining two or more materials with different characteristics one can get a diversity of properties that usually an isolated material can not. Generally speaking, one can get advantageous rigidity with very little expense on weight.
Sandwich panels are built by attaching two thin and rigid skins to a thick and lightweight core and even though this core usually has low rigidity it can be very beneficial in energy absorption which will be discussed in this thesis.
As said before, cellular materials play an important role in the energy absorption, for this reason this thesis will focus on the finite element simulation of cork and respective model tuning which can give engineers a better idea on the substitution of synthetic cores by this natural and recyclable one.
Cork presents itself as viable option because it is known for excellent properties in vibration control applications (vibration energy absorption), acoustical absorbent and its capacity to absorb multiple impacts with very little damage.
Using this material opens doors not only to the usage of a sustainable material but also a way to improve even more the cork economy in Portugal which is placed in the front line of use and exportation of this material.

1.2 Topic Overview

The best way to begin a thesis on a particular subject is to review some of the work done over the last years. This way one can make sure that no work will be repeated but even more important take notice of the available tools, knowledge, methods and so on.
Beginning in 2004 Lorna K. Gibson [2] wrote about the biomechanics of cellular solids, in particular the natural ones that can be mechanical efficient. Cork for example with a honeycomb structure can exhibit an exceptional behaviour in resisting buckling and bending.One important derivation of this work is that, numerically, honeycomb models give a good description on the dependence of the stiffness and strength on the loading direction.
One year later, S. P. Silva, M.A.Sabino, E.M.Fernandes, V. M. Correlo, L.F.Boesel and R. L. Reis [3] reviewed the cork chemical composition, physical and mechanical properties, capabilities and applications. Some properties of natural cork and agglomerates are presented and compared with other synthetic materials providing a good basis for choosing foams in function of the application. It is also

concluded that in fact cork can compete with synthetic foams but within limits. Generally speaking foams with rigid wall cells offer good resistance to loads and are very good energy absorbent.

In 2006 J.S.S. Lopes, R.A.S. Moreira and J. Dias Rodrigues [4] presented in a conference an article on Experimental Identification of Dynamic Properties of Cork Compounds. With the presented procedure some of the properties essential to fully characterize cork in a numerical model are derivable, namely the storage modulus and loss factor. The experimental setup provided the wanted results for different cork compounds and presented essential information for the design of passive damping devices. One other important result from this article is the influence of cork's density and grain size in the storage modulus and loss factor. On the same year F. Teixeira Dias, V. Miranda, C. Gameiro, J. Pinho da Cruz and J. Cirne [5] developed a study on aluminium foam and agglomerated cork filling metallic tubular energy absorption devices. The conclusion stated that aluminium foam has better performance in absorbing energy but a lower specific energy absorption ratio due to its higher density.

In 2007 J.F. Mano [6] studied the creep recovery behaviour of cork under compression at different temperatures from 0°C to 50°C, he derived an hyperbolic-sine equation that describes this kind of behaviour. Also, there is always a fraction of permanent strain even if the loading is within elastic limits. Still in the same year C.P. Gameiro and J. Cirne [7] performed analysis on dynamic Axial crushing of short and long circular aluminium tubes with agglomerate cork filler. This study proved once more the capability of this kind of structure in absorbing energy from impact and its high dependence on the structure geometry. It is suggested the application of cork agglomerates to structures where an energy absorption material with low density, low cost and low strain rate sensitivity is needed.

In 2008 Pedro Carvalho [8] developed his master thesis on the analysis of mechanical behaviour and identification of failure type in sandwich structures with cork cores. This behaviour, when subjected to compression, shear and three point bending proved the rupture in the agglomerate mostly between grain (in the adhesive) which can be improved with better production procedures. Also Mariana Santos [9] studied the structural application of cork to improve the passive safety in impact cases showing once again that cork can compete with synthetic materials. In this case cork agglomerate, IMPAXX^{TM}, polyurethane foam and aluminium foam were tested showing that in terms of acceleration peak, agglomerate cork and aluminium foam have the lower ones, in terms of absorbed energy, cork comes in the second place, right after IMPAXX^{TM}. One interesting conclusion of this thesis was the developing of an index related to the energy absorbing capabilities of different materials and the verification that cork agglomerate can withstand multiples impact with litte deteriorations which is not the case of other conventional foams. Still on the same year Paulo Antunes [10] developed a Phd thesis on a constitutive model of cork-polyurethane gel composites . The model described hysteresis cycles for uniaxial compression giving a good accordance with the Finite Element Method developed in ABAQUS®. Still in 2008 João Lopes [11] modelled the dynamic behaviour of laminate structures with cork compounds for use in passive damping devices. An experimental procedure for evaluate shear storage modulus, loss factor and extensional storage modulus was made.

In 2009 Luís Paulo [12] studied the Passive and Active Flutter Suppression Concepts for Aeronautical Components with cork compounds in sandwich composites. The conclusion was that cork can indeed

provide the same flight envelope but with a lighter structure representing a big advantage in aviation. Nádia Franco [13] studied the addition of cork's agglomerate to carbon fibre/epoxy laminated in static and dynamic tests. With this work it was possible to determine the effects of the grain size and orientation of the laminate in the mechanical properties of the final sandwich. In a general way it was found that the dynamic properties of the sandwich is improved by the addition of the agglomerate, however the static properties are worse than for carbon-epoxy laminate alone. As to the impact tests developed in this thesis the conclusion dictate that the cork agglomerate can delay the delamination of the composite. Cláudia Nunes [14] on the same year studied low velocity impacts in sandwich structures. Sandwich panels with carbon faces and cork core were tested to impact trying to evaluate impact strength and damage tolerance. It was concluded the advantage of cork relative to other synthetic materials. Cork composites have a bigger resistance to impact when compared to Rohacell® once they supported bigger loads with smaller damages, however the increase in Rohacell® absorbed energy with the increase in the impact energy is bigger than for cork. Still in 2008 Osvaldo Castro, José M. Silva, Tessaleno Devezas, Arlindo Silva and Luís Gil [15] studied the optimization of the cork's properties on composites sandwiches for uses in specialized applications. With this work it was concluded that the properties of cork depends on its density, grain size and bonding procedure. Having this conclusion in mind one can adjust this parameters in order to get the intended final properties. To finalize 2008 Luís Reis and A. Silva [16] studied the mechanical behaviour of sandwich structures using natural cork agglomerates as core materials. The main objective was to analyse the viability of cork use in aeronautical and aerospace applications. The conclusions were that for the most of the properties, the cork, has still plenty of room for improvements when compared with other commercial and synthetic materials.

In 2010 Luís Bom [17] performed a numerical study on the behaviour of cork subjected to compression and tension. The main aim was to develop numerical models to the microscopic scale and from there conclude the Young modulus of the cell's wall constituent and finally the Young modulus of the agglomerate. The results were in general satisfactory and lead to the conclusion that the isotropy of agglomerate cork is caused by industrial processes. Also in the same year Rodrigo Coelho [18] studied the development of passive protective systems using cellular materials. The aim was the integration of agglomerate cork in the role of energy absorption from impact in road helmets. The feasibility of mixing polystyrene with the agglomerated cork in helmets was analysed and tested numerically, concluding that EPS has better properties regarding impact however in the case of a violent impact the EPS will deform and lose its capability to absorb energy making the use of cork very interesting for multi impact once it tends to recover its initial shape.

In 2011 Manuel Píriz [19] studied on the possibility of cork's agglomerate use in passive vibration control of aerospace structures. The conclusion was that this viscoelastic material, with its low weight and low price could indeed have a great potential in various aeroelastic phenomena. S. Sanchez-Saez, E. Barbero and J. Cirne [20] still in 2011 examined the hight speed impact in agglomerated cork structures. Three types of specimens were constructed, one of agglomerated cork, one made of two thin spaced layers of aluminium sheet and a sandwich structure of aluminium sheet and agglomerated cork core. The results dictated that the agglomerated cork has not a big influence in the ballistic limit of the struc-

ture but could in fact increase significantly the impact absorbed energy.
In 2012 Joana Sousa [21] studied the Blast-wave absorption capacity of sandwich structures incorporating cellular materials. A numerical model was developed and good correlation with the experimental results was achieved. Also it was concluded that the core of the sandwich structure was responsible for 80% to 90% of energy absorption.
In 2013 Romina Fernandes [22] developed a study on the fracture behaviour of carbon/epoxy-cork composite. With this study it was verified an increase on the interlaminar toughness in mode I. Relative to mode II a continuous increase of energy was verified with the crack propagation. Still on the same year João Lopes [23] studied the effects of design parameters on damping of composite materials for aeronautical applications. The results of this thesis proved the possibility of using cork as a viable passive solution to improve the damping properties of high performance composites, in fact, the inclusion of cork in the composite give rise to an increase of the loss factor as well as a change of the natural frequencies of the structure according to the design requirements for a particular application. Georgino Serra [24] get his master thesis on the impact response on sandwich panels. It was noted that as the impact energy increase, the reinstituted energy diminish and consequently bigger damage to the material. In a laminate this relation is almost linear but in the sandwich panels this is not true. Also, M. Costas, J. Díaz, L.E. Romera, S. Hernández and A. Tielas [25] studied on the static and dynamic axial crushing analysis of car frontal impact hybrid absorbers. The results showed an improvement in terms of energy absorption of all the steel-padding specimen in comparison with the original piece, however when it comes to efficiency, the simulations on tube with corrugated CFRP insert and cork-filled tube does not worth the increase in mass. Hugo Policarpo [26] developed numerical and experimental models for vibration attenuation using cork composite materials.
In 2014 Tiago Castilho [27] studied the impact resistance of marine sandwich structures. Four different core materials were tested (PVC, Balsa, Corecork NL10 and NL20) and used to produce a sandwich laminated with E-glass/polyester skins. This thesis indicated that cork sandwich composites have potential in applications with impact requirements, however the stiffness is low and the weight high. Also in 2014 F.A.O. Fernandes, R.J.S. Pascoal and R.J. Alves de Sousa [28] modelled impact response of agglomerated cork. This work simulated cork's compressive behaviour when subjected to impact including the material's relaxation after the dynamic compression. The numerical simulations were performed using FEA and the material model developed was validated with success against experimental results. It was concluded that agglomerated cork has a great potential in energy absorption applications and also verified that agglomerated cork has a great capability of returning elastically, mainly at dynamic strain rates where the permanent deformation was almost none. Showing once again that agglomerated cork can be used in devices where re utilization is necessary after the first impact.
In 2015 S. Sanchez-Saez, E.Barbero, S.K.Garcia-Castillo, I.Ivañez and J.Cirne [29] experimentally tested the response of agglomerated cork under multi-impact loads. A high percentage of the impact energy was absorbed for the impact energies studied and was also verified that the absorbed energy increase with the impact energy .This work verified once more that agglomerated cork has excellent energy-absorption capabilities since the absorbed energy can be considered independent of the num-

ber of impacts.
Conluding this topic overview in the current year of 2016 Yie Sue Chua, Elliot Law, Sze Dai Pang and Ser Tong Quek [30] beginning with the idea that fish scale structures resist penetration when subject to localized impact and that cellular materials such as cork are lightweight and have good energy absorption capacity decided to combine both concepts expecting the creation of a composite structure with improved performance against low-velocity impact. The conclusions were that the specimens with curved scales produce the lowest peak stress transferred and out-perform sandwich specimens with the same volume of materials. In addition, it was concluded the existence of an optimum range for the stiffness and strength of the scales relative to the underlying layer for effective dissipation of the impact energy and minimal stresses transfer to the protected object.

1.3 Objectives

The main aim of this thesis is to understand the mechanical behaviour of cork's agglomerates when in compression at different strain rates, and model it in LS-DYNA for later use and simulation in some components where the use of this material can be advantageous.
Having the model of the material, simulations and correlations with experimental data will be done so that the model can be validated and used continuously. Beyond this, impact loading will be tested as a case study for an aeronautical component and for a generic sandwich plate with a core made of agglomerated cork.
With this in mind, the developed models will decrease experimental and expensive testing in components using cork's agglomerate with, of course, some degree of approximation.
Achieving this, it will be possible to give engineers better tools for the design process of such structures.

1.4 Thesis Outline

Briefly, the work plan for this thesis can be summarized as:

1. Topic overview, already presented, in cork applications for energy absorption purposes and numerical models - In this chapter a review of some work done on this area is made in order to situate ourselves in the current theme;

2. Introductory concepts- This will provide the theoretical tools needed to understand the results, how they were obtained and the physics behind the numerical models. Also, two specific models of cellular materials predefined in LS-DYNA will be explained from the theoretical point of view;

3. Implementation- This chapter will demonstrate what were the inputs utilized, the simulation setup and the meshes that were the basis of the thesis.

4. Results and Test cases- This chapter will be about the results obtained for the simulation of cork in compression and for the simulation of cork usage in specific components where its use could be

advantageous, also the results will be analysed and compared with the same components without cork;

5. Conclusions- Even though most of the conclusions will be taken as the tests and respective results are provided, this chapter present general conclusions and limitations about the use of cork and its numerical model;

6. Future work - Finalizing this thesis one can understand what can still be done and what improvements can still be made to this material. This chapter intends to guide the future in this theme.

Chapter 2

Background

2.1 Theoretical Overview

In this part of the thesis the theoretical concepts involved will be presented for better understanding of the results and the procedures to achieve them. The fundamental theme involved is the cellular materials one.

2.1.1 Cellular Materials

Cellular materials applied to energy absorption problems are the basis of this thesis. Saying this, a basic understanding of cellular materials mechanics is fundamental. This kind of material has a wide range of applications and can be found in many sceneries as for example in animals and human bodies whose bones are itself cellular materials.
Mechanically speaking there are 2D prismatic cells or honeycomb and 3D polyhedral cells also called foams.

The basic characteristics of this kind of materials are:

1. Lightweight;

2. Can undergo large deformations at constant stress;

3. Low thermal conductivity;

4. Large surface area.

As an example of cellular materials take notice of the figures 2.1 showing artificial honeycombs and 2.2 showing natural cellular materials:

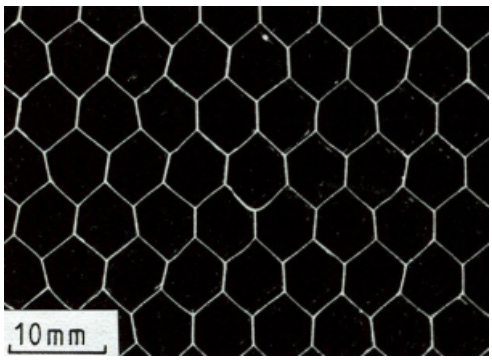

(a) Aluminium Honeycomb

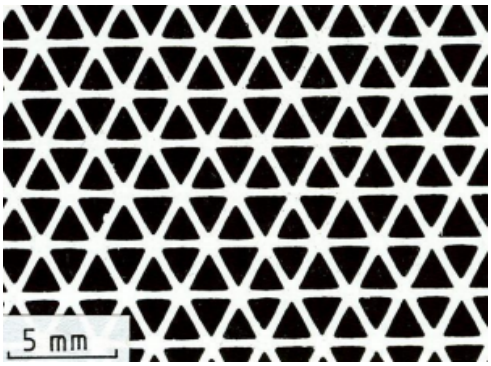

(b) Ceramic Honeycomb (Isogrid®)

Figure 2.1: Artificial cellular Materials (Source [31])

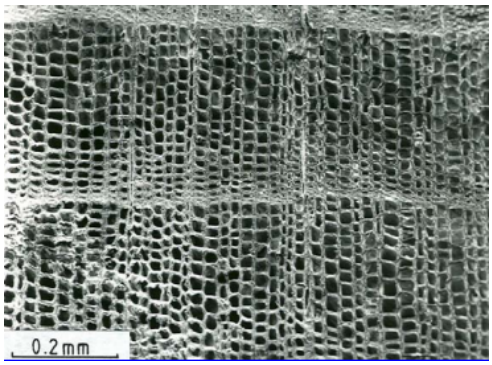

(a) Ceddar wood

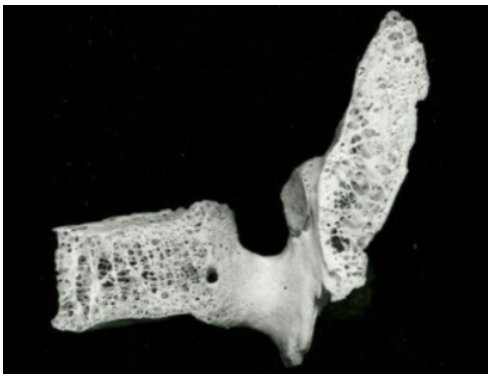

(b) Vertebral bone

Figure 2.2: Natural cellular Materials(Source [31])

Even though this material is very useful for many application, there is still plenty of room for improvement once their behaviour is different from the one common materials have. In the case of numerical simulation there are a huge need to have experimental data from tests to fully characterize this behaviour and consequently correct results. The properties needed to characterize this material depends on many factors, some of them can be enumerated in the following list:

1. Properties of the solid by which it is constituted: E_s,ρ_s,σ_{ys}, etc;

2. Cell geometry;

3. Cell shape;

4. Open or Closed cell;

5. Cell size;

6. Relative density given by equation 2.1

$$\frac{\rho^*}{\rho_s} = \frac{M_s}{V_T}\frac{V_s}{M_s} = \frac{V_s}{V_T} = 1 - porosity \tag{2.1}$$

Where ρ^* is the density of the cellular material, ρ_s is density of the material of which it is made of, V_T is the total volume, V_s is the volume occupied by the solid part and M_s is the mass. It is important to note that as the relative density increases the cell's walls thicken and the pore volume decreases. As said before the geometry of the cell is a very important factor for the final properties. Figure 2.3 is an example of a geometrical characterization.

The full characterization of the cellular material geometry gets out of the scope of this thesis. For

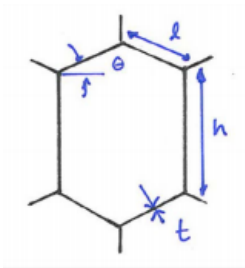

Figure 2.3: Cell (Source [31])

detail about this theme one can acess the class notes from [31], however it is interesting to note that the modelling of cellular materials for structural analysis can be made by three different approaches:

1. Unit cell;
2. Dimensional analysis;
3. Finite element analysis.

Honeycomb in plane behaviour

In plane behaviour of honeycombs materials in compression has three different regions, one linear elastic where the cells bend, one stress plateau where the cells are subjected to buckling, yielding and brittle crushing and the last region of densification where the cell's walls finally touch. This behaviour, shown in the figure 2.4 is typical from cellular materials and it is also responsible for the high energy absorption characteristics.

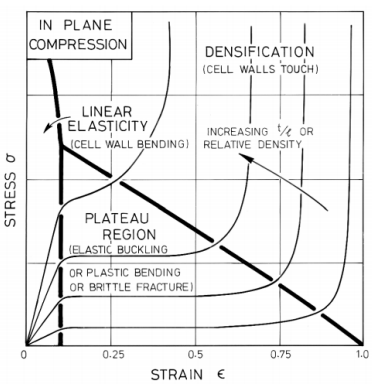

(a) Cellular material in compression

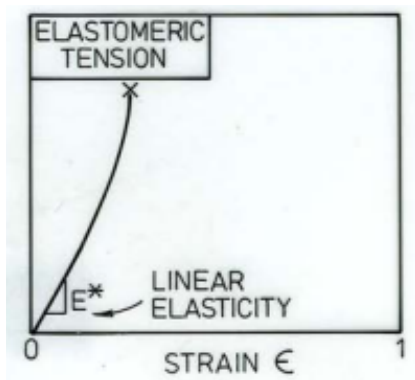

(b) Cellular material in tension

Figure 2.4: Cellular Materials Behaviour (Source [31])

It is important to note that all the best properties of cellular materials exist provided that it is used mainly in compression. As can be seen in the figure 2.4 b), this kind of material, when in tension fractures at very low strains. It is possible however the existence of a short plateau when the cell's walls are capable of yielding in tension. For the characterization of this material, there is some degree of approximation. In this particular case there is the need to assume:

1. t/l small ($\frac{\rho^*}{\rho_s}$ small) that permits to neglect axial and shear contribution to the overall deformation;

2. Small deformations;

3. Cell walls behave as a linear elastic and isotropic material;

4. Symmetric geometry when rotated 180 degrees about each of three mutually perpendicular axes.

With this assumptions in mind it is possible to derive the matrix 2.2 that rules the behaviour in the linear region.

$$\begin{bmatrix} \epsilon_{11} \\ \epsilon_{22} \\ \epsilon_{33} \\ \epsilon_{23} \\ \epsilon_{13} \\ \epsilon_{12} \end{bmatrix} = \begin{bmatrix} \frac{1}{E_{11}} & \frac{-v_{21}}{E_{22}} & \frac{-v_{31}}{E_{33}} & 0 & 0 & 0 \\ \frac{-v_{12}}{E_{11}} & \frac{1}{E_{22}} & \frac{-v_{32}}{E_{33}} & 0 & 0 & 0 \\ \frac{-v_{13}}{E_{11}} & \frac{-v_{23}}{E_{22}} & \frac{1}{E_{33}} & 0 & 0 & 0 \\ 0 & 0 & 0 & \frac{1}{G_{23}} & 0 & 0 \\ 0 & 0 & 0 & 0 & \frac{1}{G_{13}} & 0 \\ 0 & 0 & 0 & 0 & 0 & \frac{1}{G_{12}} \end{bmatrix} \begin{bmatrix} \sigma_{11} \\ \sigma_{22} \\ \sigma_{33} \\ \sigma_{23} \\ \sigma_{13} \\ \sigma_{12} \end{bmatrix} \tag{2.2}$$

In the matrix 2.2 ϵ, E and σ are the strain, Young modulus and stress respectively and the indices 1,2,3 are the directions. Of course there is the necessity to calculate the equivalent properties along the respective directions but once again this kind of calculation gets out of the scope of this thesis. If the reader has the interest in this one can consult the lecture notes from [31]. In the plateau region the main phenomena ruling the behaviour of the material is the elastic buckling of the cell's walls given by the Euler buckling load presented in the following equation 2.3.

$$P_{cr} = \frac{\omega_1^2 \pi^2 E_s I}{h^2} \tag{2.3}$$

Where P_{cr} is the Euler critical load, ω_1 is an end constrain factor, E_s is the Young modulus of the solid walls, I is the inertia moment of the section and h is the length of the biggest side of the cell.
The resulting stress at the plateau for elastic buckling that is the behaviour of cork as an example is given in equation 2.4.

$$(\sigma_{el}^*)_2 = \frac{P_{cr}}{2lcos(\theta)b} \tag{2.4}$$

Where *l* is the length of the smallest side of the cell and θ is the angle between the smallest and the biggest cell's side and b is the cell height.
In the densification region, as the walls of the cells touch each other, the material properties tends to the properties of the solid by which the walls are constituted.

Honeycomb out of plane behaviour

When honeycombs are used in absorbing energy from impact for example, they are loaded in the axial direction once in this direction the material is much more stiff and stronger. Once again the derivation of the equivalent properties along the axial axis of the cell is out of the scope of this thesis but it is useful to know that Euler buckling load is again involved in the process and given by the equation 2.5.

$$P_{cr} = \frac{\omega_2 E_s t^3}{1 - \upsilon_3^2 h} \tag{2.5}$$

Where ω_2 is an end constrain factor that depends on the stiffness of the adjacent walls, t is the thickness of the walls and υ_3 is the Poisson coefficient in the axial direction. The elastic buckling stress is given by the equation 2.6.

$$(\sigma_{el}^*)_3 = \frac{P_{cr}}{1 - \upsilon_s^2} * (\frac{t}{l})^2 \frac{2 * l/h + 2}{(h/l + sin(\theta))cos(\theta)} \tag{2.6}$$

Where υ_s is the Poisson coefficient solid that constitutes the walls of the cells.

Foams

Foams have in general a similar behaviour to what was explained about the honeycombs. In compression there is a linear elastic region where the cells bend, the stress plateau where the cells collapse by buckling, yielding and crushing and at the end of the stress-strain curve there is the densification region. When tension is the loading in the foam there is in general no buckling , yield can occur and the fracture is in general of brittle type. One important information to have in mind is that if the foam is constituted by closed cells there will be the need to account for the trapped gas inside.

The final Young Modulus of the foam is given by the equation 2.7 and can be consulted in [31] for more details.

$$\frac{E^*}{E_s} = \phi^2(\frac{\rho^*}{\rho_s})^2 + (1 - \phi)(\frac{\rho^*}{\rho_s}) + \frac{p_0(1 - 2\upsilon^*)}{E_s(1 - \rho^*/\rho_s)} \tag{2.7}$$

In the previous equation the first term describes the cell's edge bend, the second term the face stretching and the last the gas compression. Also E^* represents the cellular material Young modulus, ϕ is the volume fraction of solid in cell edges, p_0 is the initial pressure and υ^* is the Poisson coefficient of the cellular material.

The second part of the stress strain plot is the plateau characterized by a more or less constant stress and the final region is the densification where the properties of the material tend to the properties of the material that constitute the cell's walls.

Energy absorption

There are several characteristics that make cellular materials a good energy absorbent. The requirements to perform well in this application can be enumerated in the following way:

1. Must absorb the kinetic energy of the impact while keeping the peak stress below the threshold that causes damage;

2. Direction of the impact may not be predictable which implies that there must not exist a fragile direction;

3. Light;

4. Undergo large deformations at constant σ;

5. Absorb a large quantity of energy with little increase in peak stress;

6. Foams, isotropic, can absorb energy from any direction and at the same time are light and cheap;

7. Strain rate effects can not prejudice the material absorption capacity;

As already known the energy absorbed during deformation is given by the area below a stress strain plot as shown in the figure 2.5.

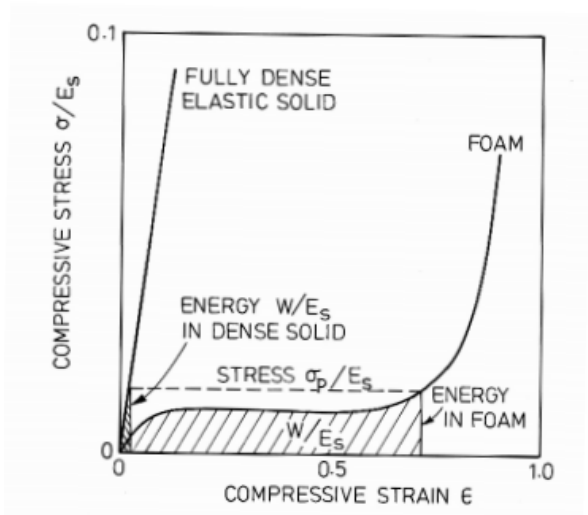

Figure 2.5: Energy absorption plot (Source [31]).

This energy absorption characteristic from cellular material is due to some mechanisms that are function of the type of the material. Take for example:

1. Elastomeric foams: Elastic buckling of cells, elastic deformation recovered and damping that dissipates energy as heat;

2. Plastic foams: Energy dissipated as plastic work or fracture with no restitution;

3. Natural cellular materials: Dissipate energy by fiber pull-out and fracture;

4. Fluid within cells: If the fluid is viscous there will be an important part of energy dissipation by this mechanism or compression of the cell content in case of closed cells.

The energy absorption can be modelled by equations 2.8, 2.9 and 2.10 for 1D.

1. Linear elastic region $\epsilon < \epsilon_0$

$$W = \frac{1}{2}\frac{\sigma_p^2}{E^*} \tag{2.8}$$

With σ_p representing the peak stress or the stress corresponding to the strain where the densification initiates.

2. Stress Plateau $\epsilon_0 < \epsilon < \epsilon_D$

$$dW = \sigma^*_{el} d\epsilon \tag{2.9}$$

Where σ^*_{el} is the stress of the elastic region limit in the cellular material.

3. At the end of plateau $\epsilon \sim \epsilon_D$ - Maximum energy absorbed just before ϵ_D, shoulder point or strain where densification initiates.

$$\frac{W_{max}}{E_s} = 0.05(\rho^*/\rho_s)^2(1 - 1/4\rho^*/\rho_s) \tag{2.10}$$

2.2 LS-DYNA Model 1- Honeycomb

The first model used to try to describe cork mechanical behaviour was the honeycomb one. There were many reasons why to believe this model could characterize cork. First there is in fact a geometrical resemblance, second there is already a few technical documents that use this model to describe cork behaviour. On the other hand there are three main reasons that make this model not so good in the present circumstances. First of all it is a complex and costly model, second the agglomerated cork is not a perfect honeycomb once the cells or aggregated of cell are randomly disposed. Lastly this model expects a lot of constants and variables that depends on many experimental tests that are often difficult to perform once costly and time consuming. The following list enumerates the inputs of this material model:

- ρ - Mass density;
- E - Young's modulus for compacted honeycomb material;
- υ - Poisson's ratio for compacted honeycomb material;
- σ_y - Yield stress for fully compacted honeycomb;
- V_F - Relative volume at which the honeycomb is fully compacted;
- μ - material viscosity coefficient. (default=.05) Recommended;
- LCA - Load curve for σ-aa versus either relative volume or volumetric strain;
- LCB - Load curve for σ-bb versus either relative volume or volumetric strain.
- LCC - Load curve for σ-cc versus either relative volume or volumetric strain;
- LCS - Load curve for shear stress versus either relative volume or volumetric strain;
- LCAB - Load curve for σ-ab versus either relative volume or volumetric strain.
- LCBC - Load curve for σ-bc versus either relative volume or volumetric strain.

- LCCA - Load curve for σ-ca versus either relative volume or volumetric strain.
- LCSR - Load curve for strain-rate effects defining the scale factor versus strain rate.
- EAAU - Elastic modulus Eaau in uncompressed configuration;
- EBBU - Elastic modulus Ebbu in uncompressed configuration;
- ECCU - Elastic modulus Eccu in uncompressed configuration;
- GABU - Shear modulus Gabu in uncompressed configuration;
- GBCU - Shear modulus Gbcu in uncompressed configuration;
- GCAU - Shear modulus Gcau in uncompressed configuration;
- TSEF - Tensile strain at element failure (element will erode);
- SSEF - Shear strain at element failure (element will erode);

The behaviour before densification is orthotropic where the components of the stress tensor are uncoupled. The elastic modulus vary, from their initial values to the fully compacted values at V_F linearly with the relative volume V_r. The equations 2.11, 2.12, 2.13, 2.14, 2.15, 2.16 describe this behaviour along the material axis.

$$E_{aa} = E_{aau} + \beta(E_{fc} - E_{aau}) \tag{2.11}$$

$$E_{bb} = E_{bbu} + \beta(E_{fc} - E_{bbu}) \tag{2.12}$$

$$E_{cc} = E_{ccu} + \beta(E_{fc} - E_{ccu}) \tag{2.13}$$

$$G_{ab} = E_{abu} + \beta(G_{fc} - E_{abu}) \tag{2.14}$$

$$G_{bc} = E_{cbu} + \beta(G_{fc} - E_{bcu}) \tag{2.15}$$

$$G_{ca} = E_{cau} + \beta(G_{fc} - E_{cau}) \tag{2.16}$$

Where E is the Young modulus, G is the Shear modulus, a, b, c are the main directions, the indice u refer to the uncompressed configuration and the indice fc refer to fully compressed. Finally β is given by the equation 2.17.

$$\beta = max[min(\frac{1 - V_r}{1 - V_F}, 1), 0] \tag{2.17}$$

At the beginning of the stress update, each element's stresses and strain rates are transformed into the local coordinate system. For the uncompacted material, the trial stress components are updated using the elastic interpolated modulus according to equations 2.18, 2.19, 2.20, 2.21, 2.22, 2.23.

$$\sigma_{aa}^{n+1(trial)} = \sigma_{aa}^{n} + E_{aa}\Delta\epsilon_{aa} \tag{2.18}$$

$$\sigma_{bb}^{n+1(trial)} = \sigma_{bb}^{n} + E_{bb}\Delta\epsilon_{bb} \tag{2.19}$$

$$\sigma_{cc}^{n+1(trial)} = \sigma_{cc}^{n} + E_{cc}\Delta\epsilon_{cc} \tag{2.20}$$

$$\sigma_{ab}^{n+1(trial)} = \sigma_{ab}^{n} + E_{ab}\Delta\epsilon_{ab} \tag{2.21}$$

$$\sigma_{bc}^{n+1(trial)} = \sigma_{bc}^{n} + E_{bc}\Delta\epsilon_{bc} \tag{2.22}$$

$$\sigma_{ca}^{n+1(trial)} = \sigma_{ca}^{n} + E_{ca}\Delta\epsilon_{ca} \tag{2.23}$$

Where n is the time step.

Each component of the updated stresses is checked to make sure that no stress exceeds the permissible values determined from the load curves. For fully compacted material it is assumed that the material behaviour is elastic-perfectly plastic and the stress components are updated following the equation 2.24.

$$s_{ij}^{trial} = s_{ij}^{n} + 2G\Delta\epsilon_{ij}^{dev(n+\frac{1}{2})} \tag{2.24}$$

where $\Delta\epsilon_{ij}^{dev}$ is given by equation 2.25

$$\Delta\epsilon_{ij}^{dev} = \Delta\epsilon_{ij} - \frac{1}{3}\Delta\epsilon_{kk}\delta_{ij} \tag{2.25}$$

A check is made to see if the yield stress for the fully compacted material is exceeded by comparing the effective trial stress to the defined yield stress, SIGY. If the effective trial stress exceeds the yield stress the stress components are simply scaled back to the yield surface. The last procedures before the final results are the update of the pressure in equation 2.26 by using the bulk modulus K given by equation 2.27.

$$p^{n+1} = p^{n} - K\Delta\epsilon_{kk}^{n+\frac{1}{2}} \tag{2.26}$$

$$K = \frac{E}{3(1-2\upsilon)} \tag{2.27}$$

The final solution or Cauchy stresses are finally given by equation 2.28.

$$\sigma_{ij}^{n+1} = s_{ij}^{n+1} - p^{n+1}\delta ij \tag{2.28}$$

Where s is the stress for the fully compressed material, p is the pressure at a given instant and δ_{ij} is the kronecker delta.

2.3 LS-DYNA Model 2-Low Density Foam

The second material model used in this thesis is the low density foam which is indeed a simpler material to use and capable to provide good results also with less computation time and experimental data. The parameters needed to characterize this model are provided in the following list:

- ρ - Mass density;
- E - Youngs modulus used in tension. For implicit problems E is set to the initial slope of load curve LCID;

- LCID - Load curve or table for the nominal stress versus strain curve definition;
- TC - Cut-off for the nominal tensile stress τ_i
- HU - Hysteretic unloading factor between 0 and 1 (default = 1, i.e., no energy dissipation);
- BETAi - Decay constant to model creep in unloading
- DAMP - Viscous coefficient (.05 ¡ recommended value ¡.50) to model damping effects;
- SHAPE - Shape factor for unloading. Active for nonzero values of the hysteretic unloading factor. Values less than one reduces the energy dissipation and greater than one increases dissipation;
- ED - Optional Young relaxation modulus,E_d, for rate effects;
- BETA1 - Optional decay constant,β_1;
- KCON - Stiffness coefficient for contact interface stiffness. If undefined the maximum slope in stress vs. strain curve is used. When the maximum slope is taken for the contact, the time step size for this material is reduced for stability. In some cases Δt may be significantly smaller, and defining a reasonable stiffness is recommended.

The compressive behaviour under uniaxial loading is assumed not to couple in the other directions. In tension the material behaves in a linear fashion until tearing occurs. This model uses tabulated input data for the loading curve where the nominal stresses are defined as a function of the elongations, ϵ_i, which in return are defined in terms of the principal stretches, λ_i, as shown by the equation 2.29.

$$\epsilon_i = \lambda_i - 1 \tag{2.29}$$

After solving for the principal stretches, the displacements are computed and if they are compressive, the corresponding values of the nominal stresses, τ_i are interpolated.

If the displacements are tensile, the nominal stresses are given by equation 2.30.

$$\eta_i = E\epsilon_i \tag{2.30}$$

And the Cauchy stresses in the principal system are calculated through equation 2.31.

$$\sigma_i = \frac{\eta_i}{\lambda_j \lambda_k} \tag{2.31}$$

The final step is to transform the stresses load back to the global system for nodal calculations. One important aspect of this thesis is the rate dependence of the material. This way it is important that the chosen model take into account this kind of phenomena. This is done through linear viscoelasticity by a convolution integral in the equation 2.32.

$$\sigma_{ij}^r = \int_0^\tau g(\tau) \frac{\partial \epsilon_{kl}}{\partial \tau} d\tau \tag{2.32}$$

Where $g(t)$ is the relaxation function. The final stress given by equation 2.33 is the contribution of the two components, one due to the foam itself and other to rate effects.

$$\sigma_{ij} = \sigma_{ij}^{f} + \sigma_{ij}^{r} \tag{2.33}$$

Since only the simple rate effects are included the relaxation function becomes given by equation 2.34.

$$g(t) = E_d e^{-\beta\tau} \tag{2.34}$$

For more information about this model one can consult [32].

Chapter 3

Implementation

Now that the fundamental concepts behind the theme of this thesis are explained it is possible to explain what inputs and meshes were used to obtain results and what test were made in order to validate the material model that was used in the case studies. The test used is a simple compression test made on a cylindrical specimen of 17,5mm of radius and 7mm high. Once the specimen is axisymmetrical one can take advantage of this fact and model only one quarter of the specimen in order to reduce the number of elements (axisymmetric analysis). Care must be taken in imposing symmetry constrains in the inner walls where the normal deformations are not allowed. This can be advantageous not only in the early stages where the reduced number of nodes and elements reduce the time spent on the simulation but also in the stage of mesh convergence where the number of elements can be kept always low. A schematics of the test and of the specimen can be seen in figures 3.1a) and 3.1b) respectively.

(a) Compression test (Source [33])

(b) Specimen used (Units: mm)

Figure 3.1: Schematics of the compression test and specimen used.

Once there is the need to understand the influence of the strain rate to fully characterize the mechanics of this material, it is necessary to control this parameter. This can be done controlling the velocity of the compression plate taking note of the relations 3.1 and 3.2.

$$\epsilon = \frac{L(\tau) - L_0}{L_0} \tag{3.1}$$

In the equation 3.1 $L(\tau)$ is the hight of the specimen at a given time and L_0 is the initial hight.

$$\dot{\epsilon} = \frac{d\epsilon}{d\tau} = \frac{d}{d\tau}(\frac{L(\tau) - L_0}{L_0}) = \frac{1}{L_0}\frac{dL(\tau)}{d\tau} = \frac{v(\tau)}{L_0} \tag{3.2}$$

Where $v(\tau)$ is the velocity of the compression plate at a given instance. The strain rates utilized in this thesis are quasi static here represented by 0.1 s^{-1}, 500 s^{-1} and 1000 s^{-1} which represent a velocity on the compressor plate of 0.0008 m/s 3.5 m/s and 7 m/s respectively.

3.1 Numerical Model

The first thing to do in the numerical implementation of a model is to create and mesh the body. In the present case, solid formulations explained in the appendix B.0.1 were utilized and in each case 4 progressively more refined meshes were utilized. With this meshes it was possible to study the influence of the formulation on the final results and also proceed to a convergence study in function of the number of elements that is a mandatory part of a finite element study. An important result to take from this is the influence of the element formulation and mesh refinement on the final results and in the CPU time that can be an important constrain. Hopefully at the end of all tests there will be possible to find a compromise between the quality of the results and CPU time for the purposes of the material model.

3.1.1 Mesh

There are two methodologies used to analyse the refinement degree of a determined mesh. One is to count the number of elements, a second method is to utilize a standard length of an element. The number of elements is a faster and simpler way to understand the convergence but on the other hand the length of the element can be advantageous for using in a different geometry and make sure that a mesh density with already good results is the same. Having this in mind the figures 3.2a), 3.2b), 3.3a), 3.3b) present the meshes used, the number of elements of each one and the characteristic length of the elements.

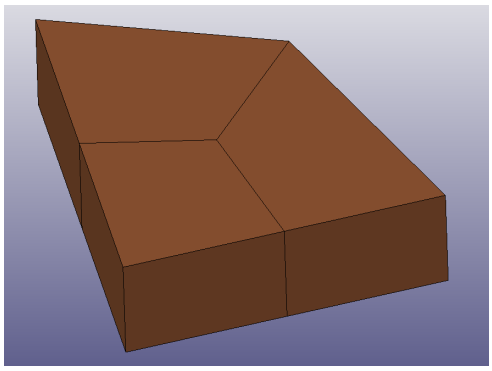

(a) Rough Mesh (3 elements/8.5mm)

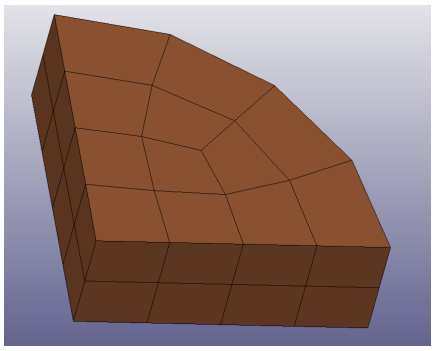

(b) Medium 1 mesh (24 elements/4mm)

Figure 3.2: Rough meshes

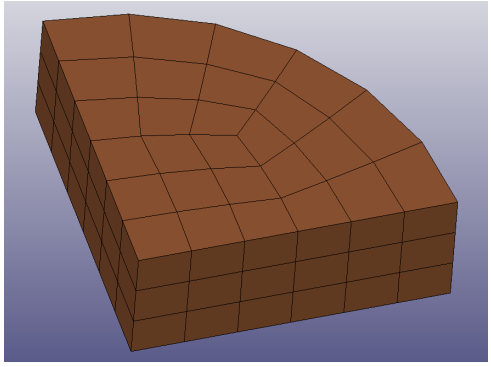

(a) Medium 2 mesh (81 elements/3mm)

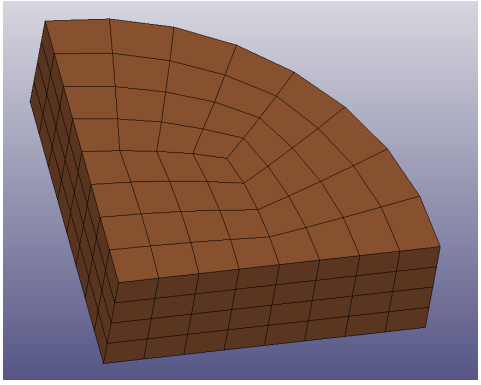

(b) Fine mesh (192 elements/2mm)

Figure 3.3: Refined meshes

3.1.2 Models Inputs

In this chapter it will be discussed experimental results used as inputs for the two models. As said before some experimental tests are expensive or even impossible to perform having in mind the resources for a project like this. The consequence of such situation is that many experimental data must be used only based on manufacturer data and other must be approximated or even estimated from similar materials which can be a huge limitation with this kind of materials.

Honeycomb

The data presented in table 3.1 was used as input of the honeycomb model.

Table 3.1: Honeycomb model inputs (Source [34])

Honeycomb		
Input	Information	Value
ρ	Density - Manufacturer Data	200 Kg/m^3
E	Young Modulus of compacted material- Cells walls material from [3]	9 GPa
v	Poisson Ratio- Cells walls material from [17]	0.30
σ_y	Estimation	6.75 GPa
Vf	Estimation	0.2
μ	Default	0.05
$BULK$	Default	0
LCA, LCB, LCC	Material assumed isotropic	Presented in figure 3.4, NL20 curve
$LCS, LCAB, LCBC, LCCA$	Material assumed isotropic	Scaled from figure 3.4, NL20 curve
$LCSR$	Value to be optimized	0
$EAAU, EBBU, ECCU, LCCA$	Material assumed isotropic and estimated from [3]	10 MPa
$GABU, GBCU, GCAU$	Material assumed isotropic and Manufacturer Data	5.9 MPa
All other parameters	Default	

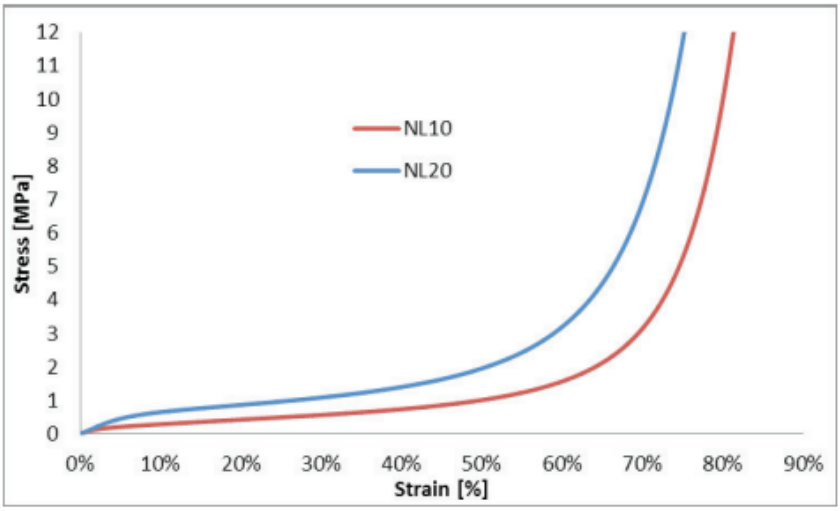

Figure 3.4: Stress vs Strain NL10 and NL20 (Source [35]).

Low density foam

The following data was used as input of the low density foam model.

Table 3.2: Low density foam model inputs (Source [34])

Low Density Foam		
Input	Information	Value
ρ	Density - Manufacturer Data	200 Kg/m^3
E	Estimated	6 MPa
$LCID$	Same as LCA	
tc	Estimation	9 GPa
hu	Estimation	1.0
β	Estimated	0.0
$damp$	Default	0.5
$Shape$	Estimated	9.0
$Fail$	Default	1.0
ed	Default	0.0
β_1	Default	0.01
$Kcon$	Default	90 MPa
All other parameters	Default	

3.2 Experimental Results

As already known, this kind of simulation do not add any value if there is no experimental results to validate de material model and verify the errors. Thanks to Amorim Cork Composites and Prof. Pedro Rosa some compression tests in cork disks were made at different strain rates. By comparing the experimental results with the simulation ones it will be possible to estimate the error of the model. Figure 3.5 presents the results obtained by Prof. Pedro Rosa in experimental testing.

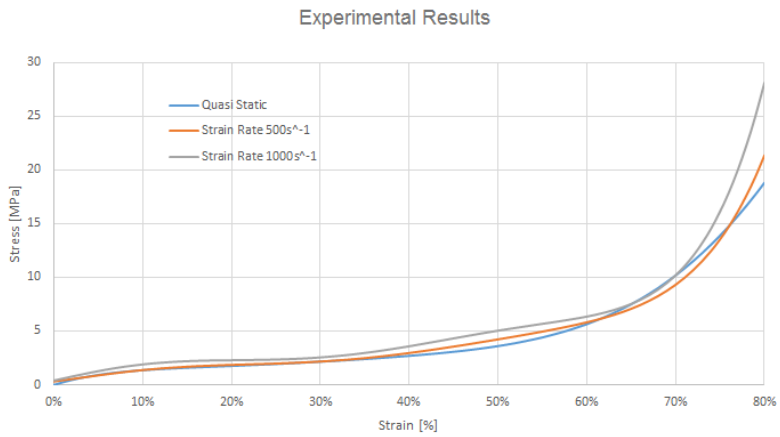

Figure 3.5: NL20 Behaviour (Prof. Pedro Rosa to Amorim Composites report).

As can be seen in the figure 3.5 the strain rate does not have great influence on the overall behaviour of the NL20 agglomerated cork once the curves are very close to each other and even small differences between experimental tests are to be expected. This characteristic can be advantageous for some applications and even for a final computational model once the parameters regarding this phenomena can be left as default. Nevertheless, this thesis pretends to develop a model the most close to reality as possible and as a consequence the parameters that describe the strain rate effects will be optimized.

Chapter 4

Results

In this chapter results from simulations using the two material models, several element formulations and 4 consecutive mesh refinements will be provided and explained in detail. In the end of this chapter it will be possible to choose the best model and apply it to three case studies. One of this case study is a 3 point bending test so that the model is pushed to the limit and noticed the fragilities of it. The second case study is the application of the model to a real world aviation component and the third is about ballistic impact on a sandwich panel of aluminium and agglomerated cork as core.

4.1 Honeycomb Results

4.1.1 Solid Formulation 1

The first simulation done was with the honeycomb model and the solid formulation 1. This choice is obvious once this material model is the most used when cork simulations are needed plus the formulation 1 is the simpler and fastest formulation.

The next figures shows important data referent to the simulation. The first figure 4.1a) presents the final behaviour of cork when in compression and respective comparative between more refined meshes and the experimental results, the second figure 4.1b) presents the error in function of the strain. This figure is very important once it permits to notice where the model needs to be refined or where the bigger error occurs. Figure 4.2 presents the hourglass graph in comparison with the total system energy. This important parameter must be controlled and maintained as close to 0% as possible once it can compromise the whole simulation. Lastly the table 4.1 presents a summary of information referent to simulation which permits to compare meshes in a more quantitative way.

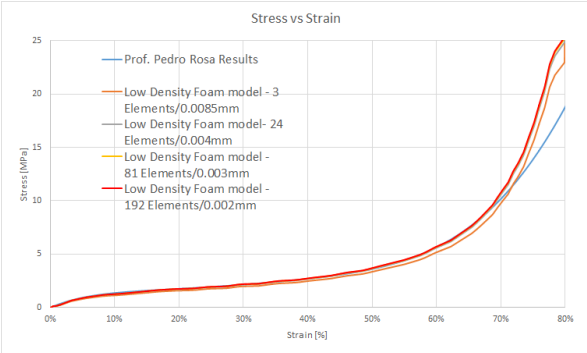

(a) Stress vs Strain

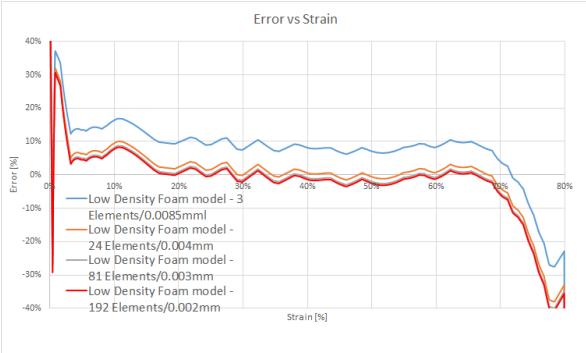

(b) Error vs Strain

Figure 4.1: Honeycomb Formulation 1 Results

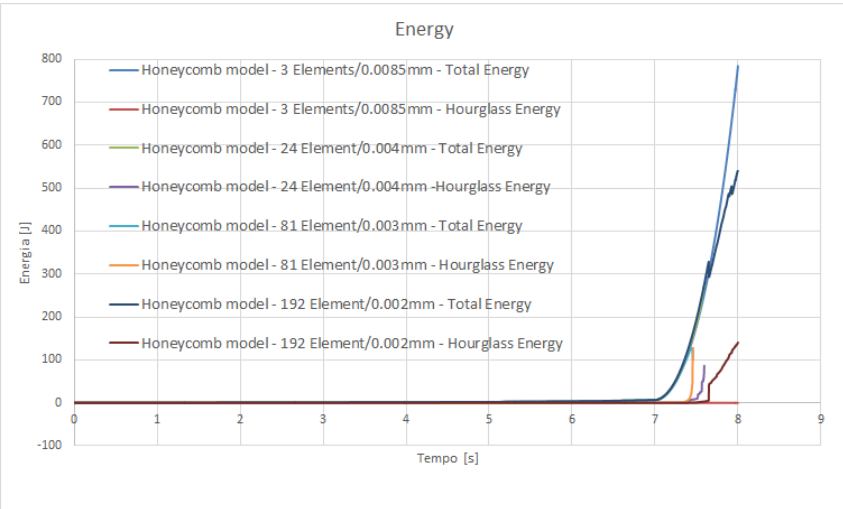

Figure 4.2: Energies vs Time of Honeycomb model form.1

Table 4.1: Simulation Information of Honeycomb form.1

Mesh	3 Element	24 Element	81 Element	192 Element Mesh
Error Elastic Region	17%	11%	9%	9%
Error Plastic Region	9%	2%	0%	0%
Error Densification Region	-5072%	-2408%	-1536%	-4483%
Avarage Error	-1735.2%	-740.8%	-453.7%	-1539.0%
Completed Simulation time	Yes	No	No	Yes
CPU time	1097s	3633.4s	7810.9s	17928s
$(Hourglass/TotalEnergy)_{max}$	0%	32%	125%	26%

The results from this simulation shows a global tendency to the convergence at least in the elastic and plastic region. In the densification region the error gets enormous and the model do not represent the cork's behaviour by far. As can be seen in the beginning of the error figure 4.1b) with the strain there is a peak of error due to mathematical induced noise that makes the stress-strain curve from simulation starting from a value very close to zero but not zero. This almost zero value when introduced in the relative error formula induce a big value. Returning to the topic of the error in the densification region

this happens due to the lack of information to fully characterize the behaviour of cork agglomerate in this region. This can be overcame by performing experimental testing on specimens which was not possible in this thesis. The processing time, as obvious get bigger as the mesh get refined and consequently the reference element edge. This behaviour is almost linear and proves that a good agreement between processing time and error must be achieved. To finalize the hourglass is indeed a problem from 24 elements on caused by the only integration point at the center that makes the model very malleable. It was not the aim, at least at this phase to control the hourglass but to see how the formulations work in the raw state. With all data in mind, one may conclude that Honeycomb model with formulation 1 is not a good model to use, there are a lack of characterization on the densification error and the hourglass is a problem that needs to be controlled if this model shows up the best one at the end.

4.1.2 Solid Formulation -1

This simulation follows the same mould as the above simulation, the only difference is the change in formulation. Notice that for the first time there are entries in the table 4.2 that are not filled. This happens because the simulation was not capable of reaching the end due to the small time step. This happens because this time step is directly proportional to a characteristic length given by the ratio of the volume of the solid element by the biggest area of the element's faces. When the material is extremely soft and highly compressible the time step get smaller as the compression continues and the simulation tends asymptotically to the end time never reaching it. The next figures 4.3 a), 4.3 b) and 4.4 represent once again the compressive behaviour of agglomerated cork, the error in function of the strain and the hourglass energy in comparison with the total energy of the system respectively:

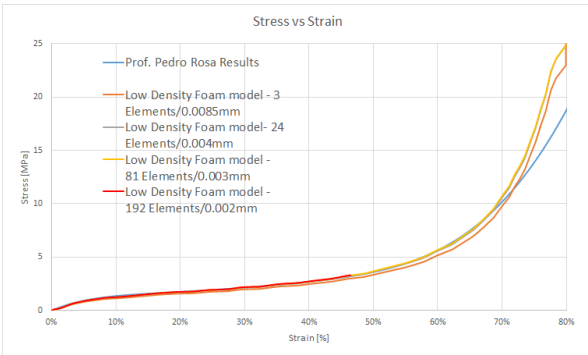

(a) Stress vs Strain

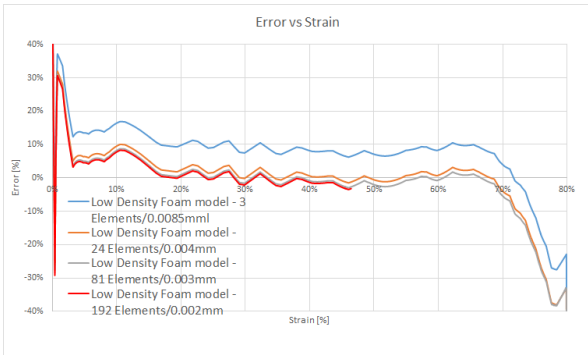

(b) Error vs Strain

Figure 4.3: Honeycomb Formulation -1 Results

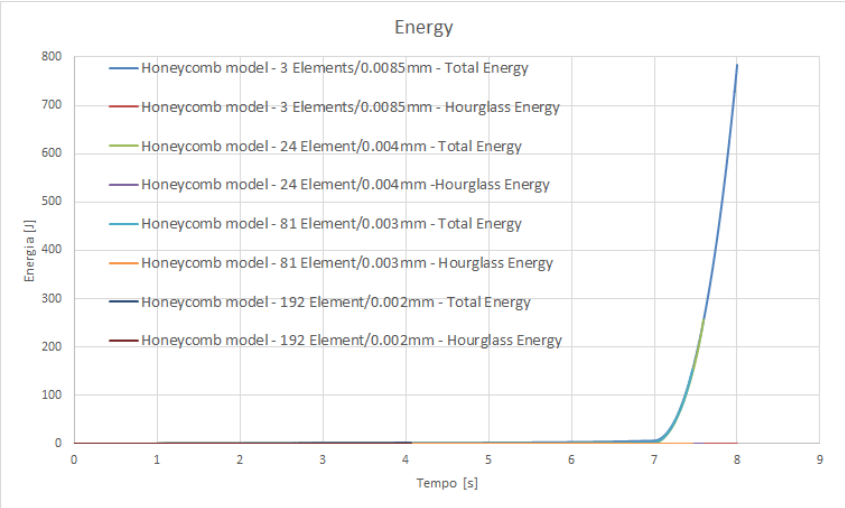

Figure 4.4: Energies vs Time of Honeycomb model form.-1

Table 4.2: Simulation Information of Honeycomb form.-1

Mesh	3 Element	24 Element	81 Element	192 Element Mesh
Error Elastic Region	17%	11%	9%	9%
Error Plastic Region	9%	2%	0%	1%
Error Densification Region	-5072%	-2417%	-1697%	-
Avarage Error	-1735.2%	-745.6%	-504.8%	-2.4%
Completed Simulation time	Yes	No	No	No
CPU time	1904s	4630.3s	15612.8s	53599.6s
$(Hourglass/TotalEnergy)_{max}$	0%	0%	0%	0%

In this situation more integration points were used and as a result hourglass is expected to be kept low. Even though the theory says that this formulation may have some hourglass tendency, the truth is that in this case this is not verified. In terms of results quality, the errors are in general better than for formulation 1 but in the densification region the error is still very large. Moreover not all the simulations were capable of reaching the end time imposed and by this reason the final strain for which experimental data is provided is not verified and the model cannot be fully validated. As this formulation is heavier than the formulation 1 so the time to process the simulation is, proving again that in this circumstances honeycomb is not a good model to describe agglomerated cork behaviour.

4.2 Low Density Foam Results

4.2.1 Solid Formulation 1

Once again all the elements from the previous simulations are presented but this time the material model is changed to Low Density Foam. The formulation 1 is used again once a new material model is choose and 1 is the simpler formulation to begin with. Figures 4.5 a), 4.5 b) and 4.6 shows the behaviour of cork, the error and finally the system's energies and the table 4.3 shows the information of the simulation.

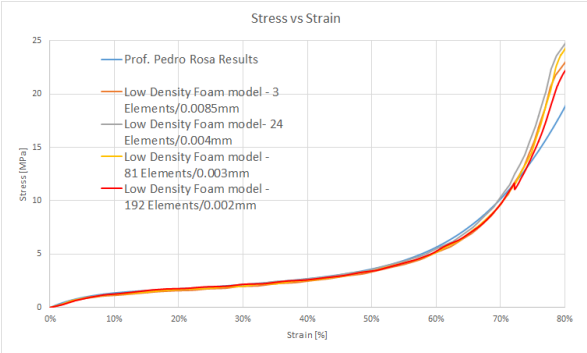

(a) Stress vs Strain

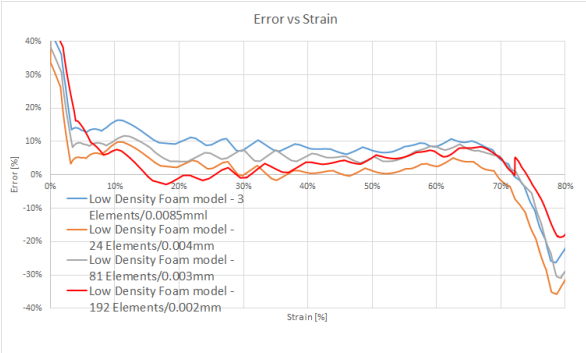

(b) Error vs Strain

Figure 4.5: Low density foam Formulation 1 Results

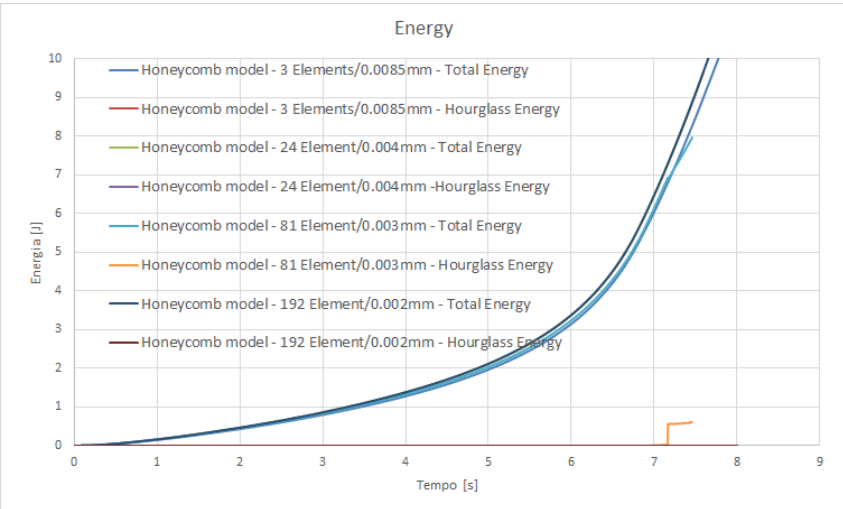

Figure 4.6: Energies vs Time of LDF model form.1

Table 4.3: Simulation Information of LDF form.1

Mesh	3 Element	24 Element	81 Element	192 Element Mesh
Error Elastic Region	20%	11%	15%	19%
Error Plastic Region	9%	2%	6%	3%
Error Densification Region	-3%	-10%	4%	2%
Avarage Error	6.3%	-1.0%	-6.3%	4.2%
Completed Simulation time	Yes	Yes	Yes	No
CPU time	101s	646s	1516s	2275.3s
$(Hourglass/TotalEnergy)_{max}$	0%	0%	0%	0%

Now that the honeycomb model in tested one can test a lighter model and experiment other formulations. The first one is the formulation 1 but contrary to what was expected there were not hourglass problems. The errors for the elastic and plateau region are in general bigger than the ones verified for the honeycomb model in the same regions and the convergence behaviour is not very clear but in the densification regions the errors become acceptable. Having in mind the increasing processing times for the increasingly refined meshes one can tell that in all occasions this model is much more lighter

than the honeycomb and it is interesting to note that is not necessary to refine the mesh more than 81 elements since 24 elements presents the lowest error and a acceptable processing time. The reason for this formulation to works so well is possibly the one point integration that makes it very good for big deformations.

4.2.2 Solid Formulation 2

For the first time formulation 2 is used. The reason why it was not utilized in the honeycomb material model is that this model is so computational heavy that the choice of heavier formulation would increase the time exponentially and this was not consistence with the time available to the development of this thesis. Figures 4.7 a), 4.7 b), 4.8 and table 4.4 presents the results for this model.

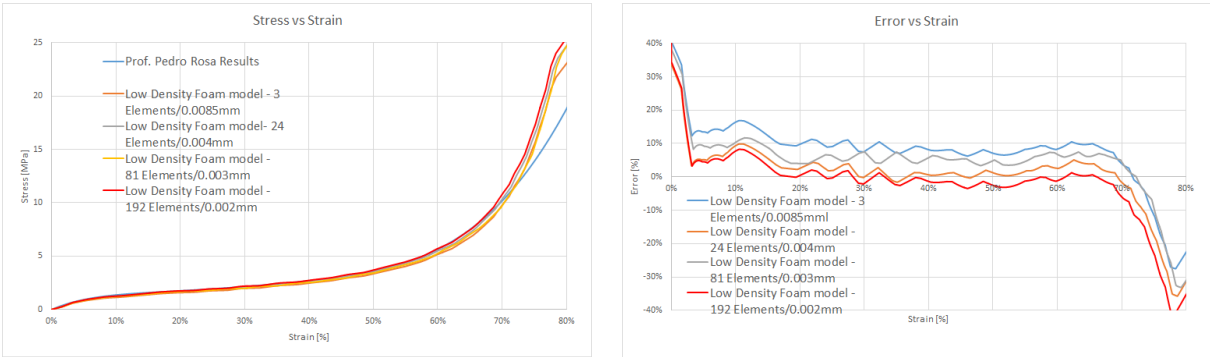

(a) Stress vs Strain

(b) Error vs Strain

Figure 4.7: Low density foam Formulation 2 Results

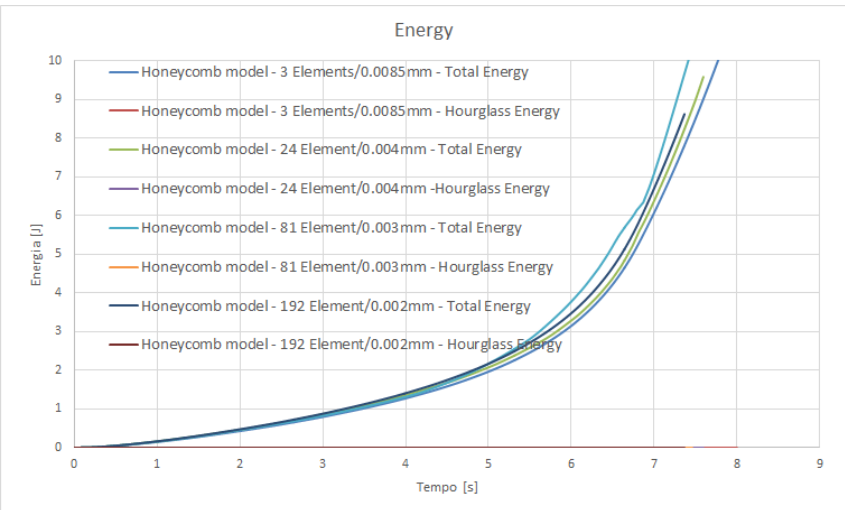

Figure 4.8: Energies vs Time of LDF model form.2

Table 4.4: Simulation Information of LDF form.2

Mesh	3 Element	24 Element	81 Element	192 Element Mesh
Error Elastic Region	19%	11%	15%	11%
Error Plastic Region	9%	2%	6%	0%
Error Densification Region	-3%	-10%	-8%	-15%
Avarage Error	6.0%	-1.0%	2.3%	-3.1%
Completed Simulation time	Yes	Yes	No	No
CPU time	155s	826s	2821.9s	4535.1s
$(Hourglass/TotalEnergy)_{max}$	0%	0%	0%	0%

This formulation is selective reduced integrate brick element, this means that there are 8 nodes but not all degrees of freedom are free to move. By what is said in the appendix B.0.1 it alleviates the volume locking but it is still not a good element for severe deformations. In spite of what was said the model ends up performing very well in terms of errors and hourglass but it has a bigger processing time.

4.2.3 Solid Formulation 3

The heavier formulation of them all was utilized, there was not a big expectation with this formulation since it is a very stiff one. One way or another it is still interesting to take notice of the behaviour of a formulation like this applied to a malleable material because this model is a fully integrated model with 6 dofs per node, good for small deformations but due to volume locking severe deformations are not well described. Although the the hourglass is 0% for all the cases as can be seen in figure 4.10 and table 4.5 not all the simulations reached the end and the errors are big and not comparable to the error of the formulation 1 and 2 as seen in figures 4.9 a) and 4.9 b). Due to the rigidity of the formulation, the model tends to initiate the densification process sooner and as consequence the time step gets smaller sooner which makes impossible for the simulation to reach the end giving a rise to the error in this region. Of course the cpu times is bigger since this formulation is the heavier of them all. Gathering all that was said this formulation when compared with other simpler and with better results can not compete.

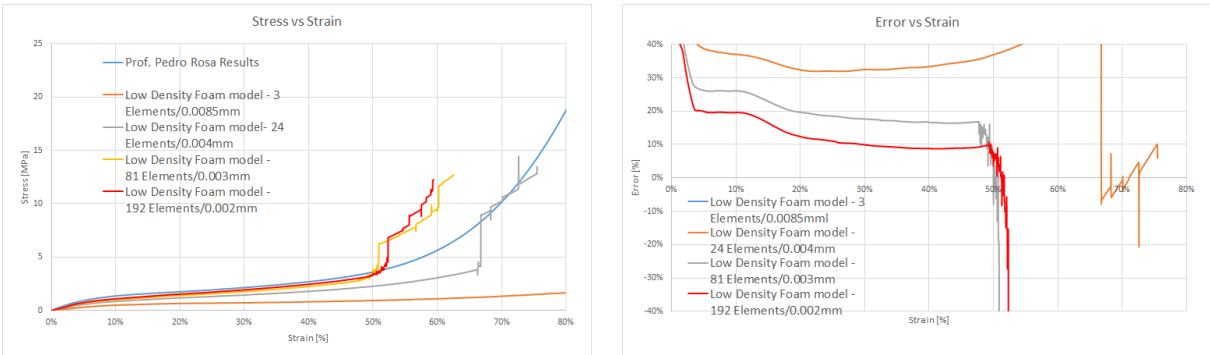

(a) Stress vs Strain

(b) Error vs Strain

Figure 4.9: Low density foam Formulation 3 Results

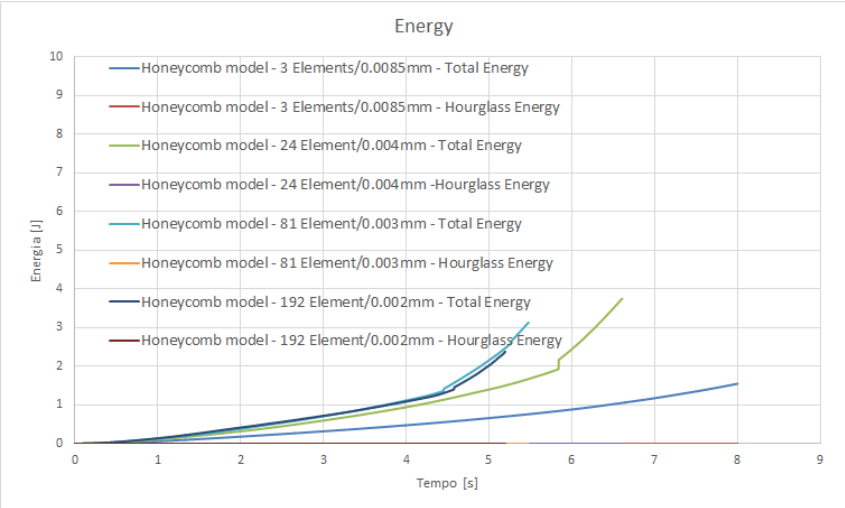

Figure 4.10: Energies vs Time of LDF model form.3

Table 4.5: Simulation Information of LDF form.3

Mesh	3 Element	24 Element	81 Element	192 Element Mesh
Error Elastic Region	68%	43%	31%	25%
Error Plastic Region	69%	35%	2%	-3%
Error Densification Region	89%	22%	98%	-
Avarage Error	75.5%	33.3%	2.9%	1.5%
Completed Simulation time	Yes	No	No	No
CPU time	226s	1230.0s	4617.9s	8936.1s
$(Hourglass/TotalEnergy)_{max}$	0%	0%	0%	0%

4.2.4 Solid Formulation -1

This time formulation -1 one was chosen. This kind of formulation is similar to type 2 but with the exception that takes in account the poor aspect ratios of the mesh. This poor aspect ration is not present in every meshes but becomes more prominent once the solid is compressed and flattened. Figures 4.11 a) and 4.11 b) show the specimen behaviour and the error, 4.12 show the energies of the system and finally table 4.6 show a the global information of the simulation.

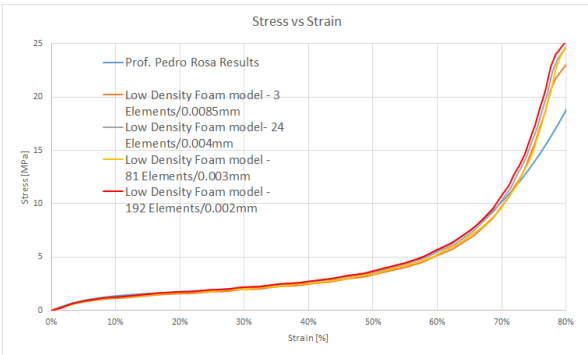

(a) Stress vs Strain

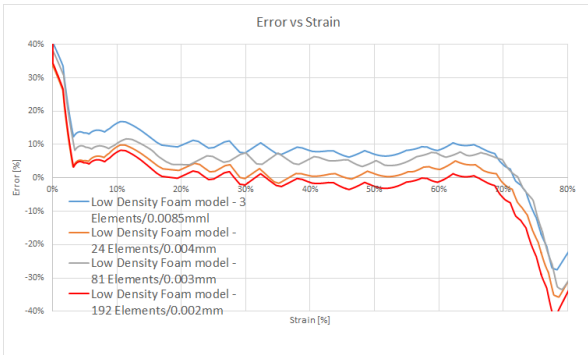

(b) Error vs Strain

Figure 4.11: Low density foam Formulation -1 Results

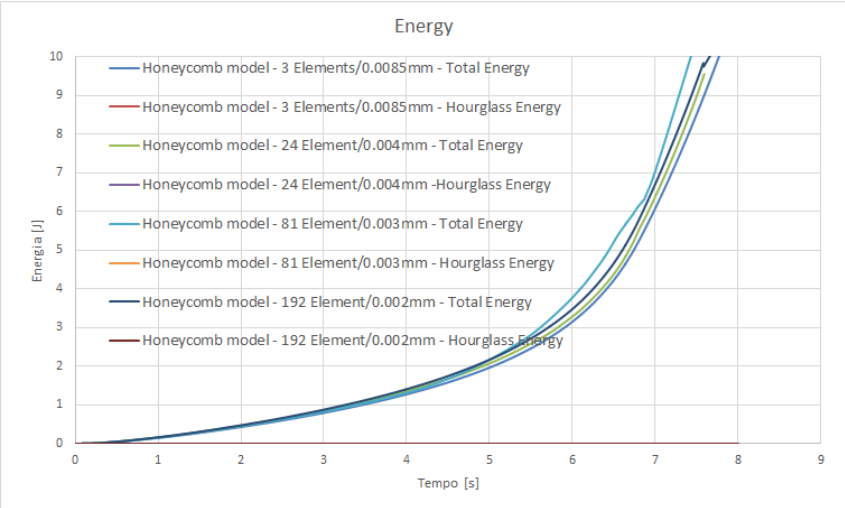

Figure 4.12: Energies vs Time of LDF model form.-1

Table 4.6: Simulation Information of LDF form.-1

Mesh	3 Element	24 Element	81 Element	192 Element Mesh
Error Elastic Region	19%	11%	15%	11%
Error Plastic Region	9%	2%	6%	0%
Error Densification Region	-3%	-10%	-4%	-7%
Avarage Error	6.0%	-1.0%	3.4%	-1.4%
Completed Simulation time	Yes	Yes	Yes	Yes
CPU time	172s	680s	2758s	6013s
$(Hourglass/TotalEnergy)_{max}$	0%	0%	0%	0%

Formulation -1 was utilized previously in the honeycomb model which not leave much to say about it. The results are in general similar to the formulation 2 with the exception of the most refined mesh where the results are a little better. There are no problems with hourglass but as a negative point the processing time is a bit bigger than for all other formulations.

4.2.5 Solid Formulation -2

For last formulation -2 was utilized, it can bes noticed by the appendix chapter B.0.1 that both formulations -1 and -2 are similar to formulation 2 but -1 is an efficient formulation and -2 is an accurate formulation. Having this two simulations, one can compare by the results presented in figures 4.13 a), 4.13 b), 4.14 and table 4.7 and understand in which way the results are affected.

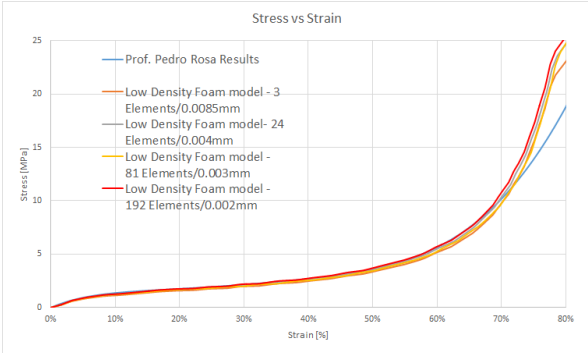

(a) Stress vs Strain

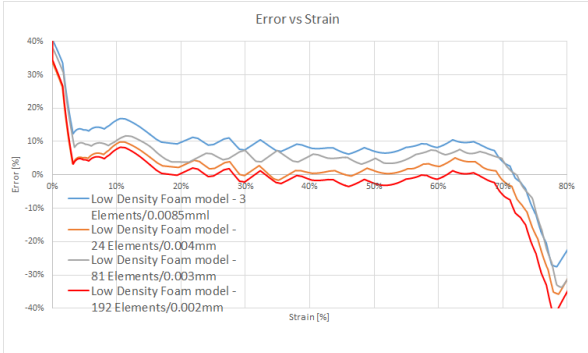

(b) Error vs Strain

Figure 4.13: Low density foam Formulation -2 Results

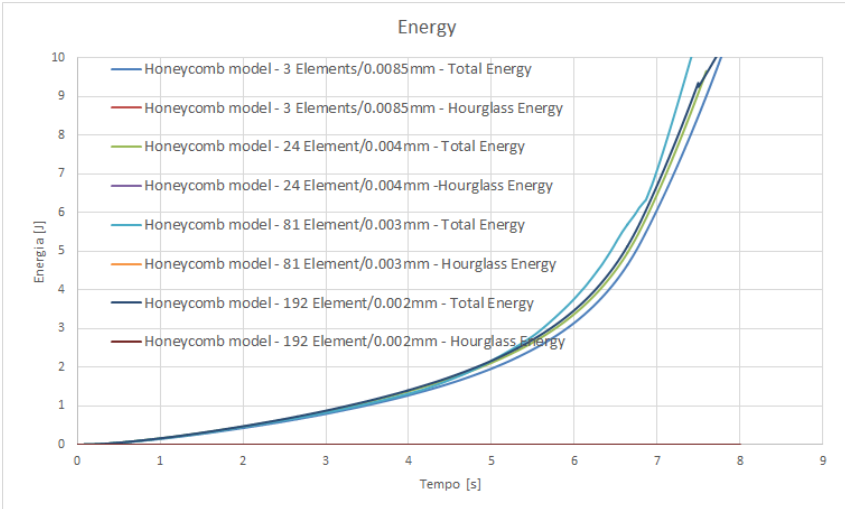

Figure 4.14: Energies vs Time of LDF model form.-2

Table 4.7: Simulation Information of LDF form.-2

Mesh	3 Element	24 Element	81 Element	192 Element Mesh
Error Elastic Region	19%	11%	15%	11%
Error Plastic Region	9%	2%	6%	0%
Error Densification Region	-3%	-10%	-8%	-6%
Avarage Error	6.0%	-1.0%	2.1%	-0.9%
Completed Simulation time	Yes	Yes	Yes	Yes
CPU time	229s	343s	4486s	12597s
$(Hourglass/TotalEnergy)_{max}$	0%	0%	0%	0%

The results are not best than the ones from the formulation -1 except for the average error for the last two more refined meshes. All the simulations were capable to get to the the end but the processing time is bigger. This model shows no added value to the formulation 1 once the simulation is more time consuming.

4.3 Model Selection

In this section the comparison between the models will be made in a more systematic way. There is a need to choose a final model to continue and tune it. It is not enough to chose the model and formulation with the smallest error, it is also necessary to find a compromise between the errors and the processing time but once the error oscillates much with the increase in the strain is useful to find the standard deviation in the errors, try to minimize it, minimizing the average error too. This can be done analysing the information in figures 4.15, 4.16, 4.17. Summing up there is the need to minimize the standard deviation, the average error and the error for all the regions but at the same time choose a model whose processing time pays of the errors and are in good agreement with engineering in real world and with the working station in use.

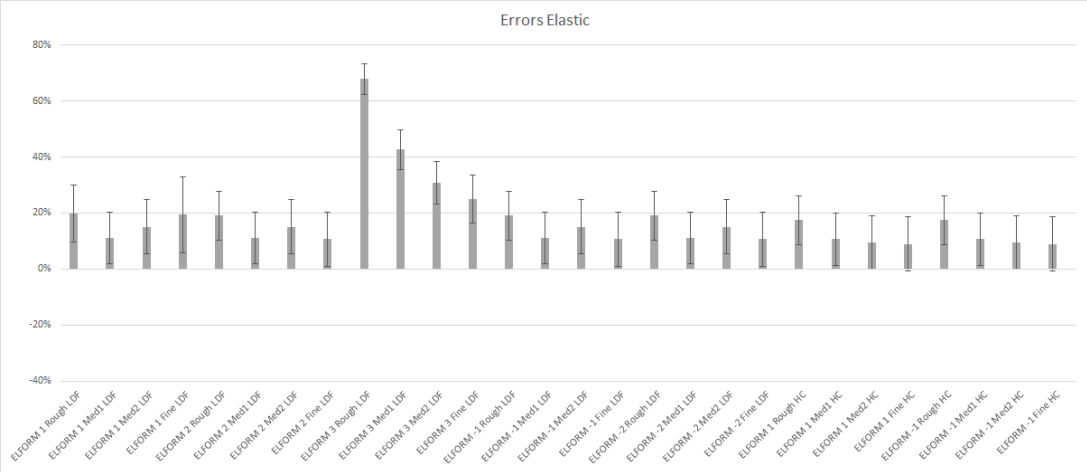

Figure 4.15: Models errors and Standard Deviation in Elastic Region

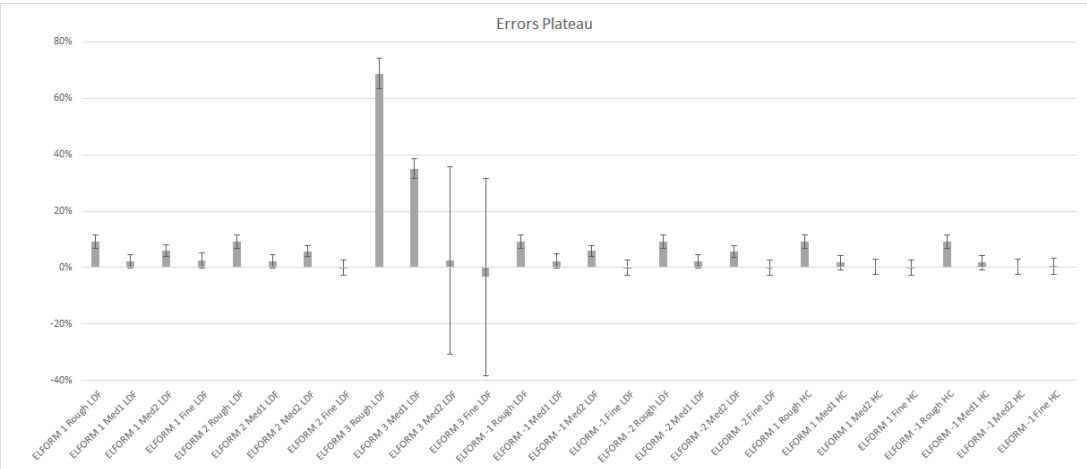

Figure 4.16: Models errors and Standard Deviation in the Plateau Region

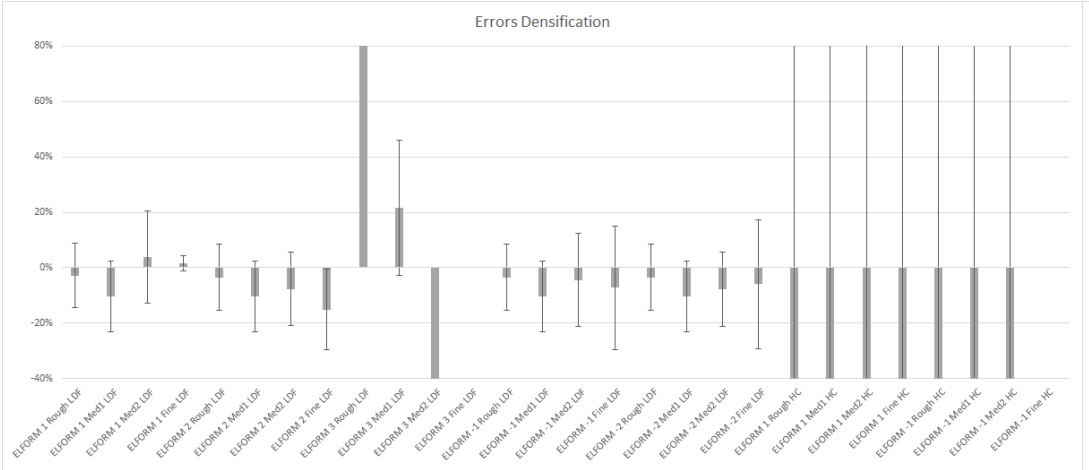

Figure 4.17: Models errors and Standard Deviation in the Densification Region

With all the information gathered it is safe to chose the Formulation 1 of the Low Density foam material model. It presents a low error with a acceptable standard deviation, plus it is a simple model with low processing time and no hourglass problems. This model is assumed to have converged to the solution as long as a mesh with the same density as the specimen is used, in this case the elements must have an edge of about 4mm. The fact that this model is not affected by hourglass doesn't mean that it won't be, the compression simulation is a very simple one and in case of using this model and mesh to other simulation care must be taken to control hourglass and maintain it between acceptable values for example 10% of the total system energy. There is still space to investigate in deep this model, for example one can try a mesh with elements between 24 and 81 once there won't be a big increase in the processing time .

4.4 Model update for strain rate effects

The methodology utilized to develop this thesis was very simple. First it would be interesting to study two material models with several solid element formulations in its raw results. When this study was done one could proceed to the fine tune of parameters used as input for the material and that were guessed in the beginning, plus cards provided by LS-DYNA to control some characteristics of the simulation may be tried. One of this parameters was hourglass but since there were no problems in this field one could ignore this parameter, the second and maybe one of the most important parameters of this thesis was to model the cork's behaviour at different strain rates. One can not forget that for many applications as for example armours the strain rate is a very important factor and generally speaking the available data for materials are provided in quasi static regime. Happily in this thesis experimental data for cork's compression at quasi static, 500 s^{-1} and 1000 s^{-1} strain rates was arranged. It was said before that values that affect the strain rate are E_d and β_1, this values were independently optimized for the different strain rates and the expectation was to find a single value to each variable that could correctly characterize the sensibility of cork to the strain rate. This model tune should have been done at the same time, this means optimize both variables at the same time and making the software optimize

them for all strain rates. As the optimization software is a freeware from LS-DYNA there are not many powerful capabilities and the one at the time approach was used. Firstly is useful to understand the behaviour of the stress-strain graph without optimized variables when other strain rates are imposed and then with the optimized variables. This can be seen and analysed in figure 4.18 and table 4.8 At 500 s^{-1} the compression plate must move at 3.5 m/s and for 1000 s^{-1} the plate moves at 7 m/s.

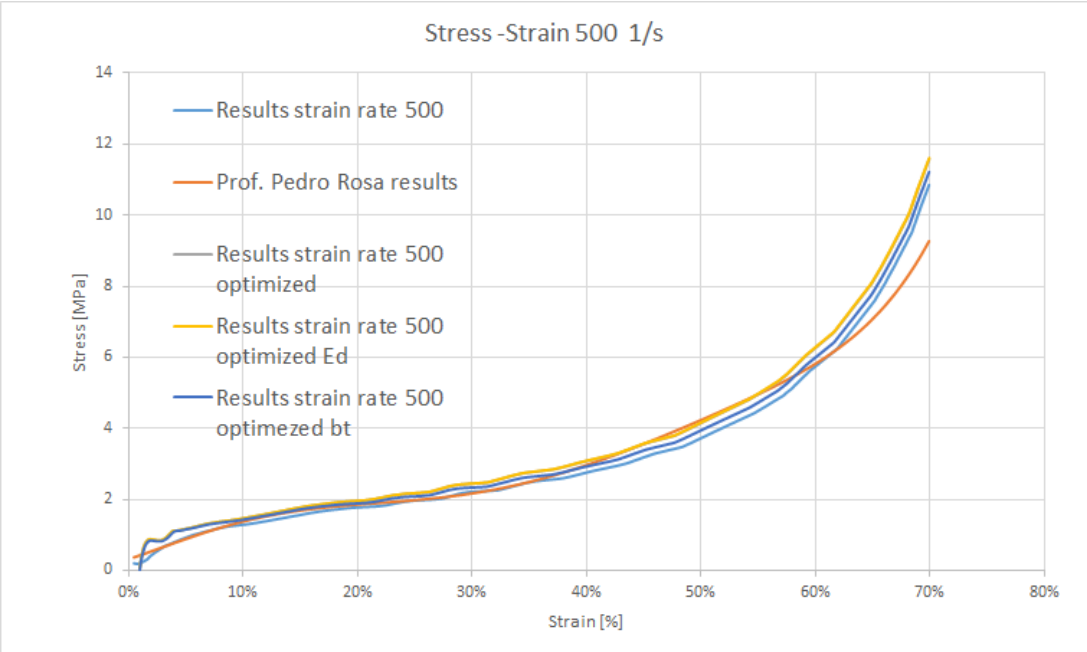

Figure 4.18: Strain Rate 500 s^{-1} behaviour

Table 4.8: Tune for 500 s^{-1}

Model	Raw model	Model Full opt.	Model with $E_d = 317434$ opt.	Model with $\beta_1 = 122$ opt.
Average error	2%	-9%	-10%	-5%
Elastic error	8%	-27%	-27%	-22%
Plateau Error	6%	-5%	-5%	0%
Densification error	-8%	-16%	-16%	-11%

From this results it is possible to conclude that the optimization didn't occur the way it should. The errors tend to increase with the optimization parameters when compared with experimental results at the same strain rate. As known optimization tools are to be used with caution, what happened in this case is that the surface generated by the objective and the variables in test found a relative minimum or maximum that the software assumed to be the best solution and stop looking. The wanted solution is a maximum or minimum but an absolute one. With all this in mind the best behaviour is the model with the original parameters. In spite of what was said one may al least conclude that the full optimized model is the second best model and that E_d is the parameter that influence the behaviour the most. The reader may be induced in error by the table once the errors for β_1 are the lowest between the optimized ones, actually this happens because the strain rate behaviour is very little influenced by this variable. One the other hand it can be seen that E_d is the parameter that introduce the biggest changes in the general

behaviour. Now it is possible to proceed to the strain rate of 1000 s^{-1} with the results presented in figure 4.19 and table 4.9.

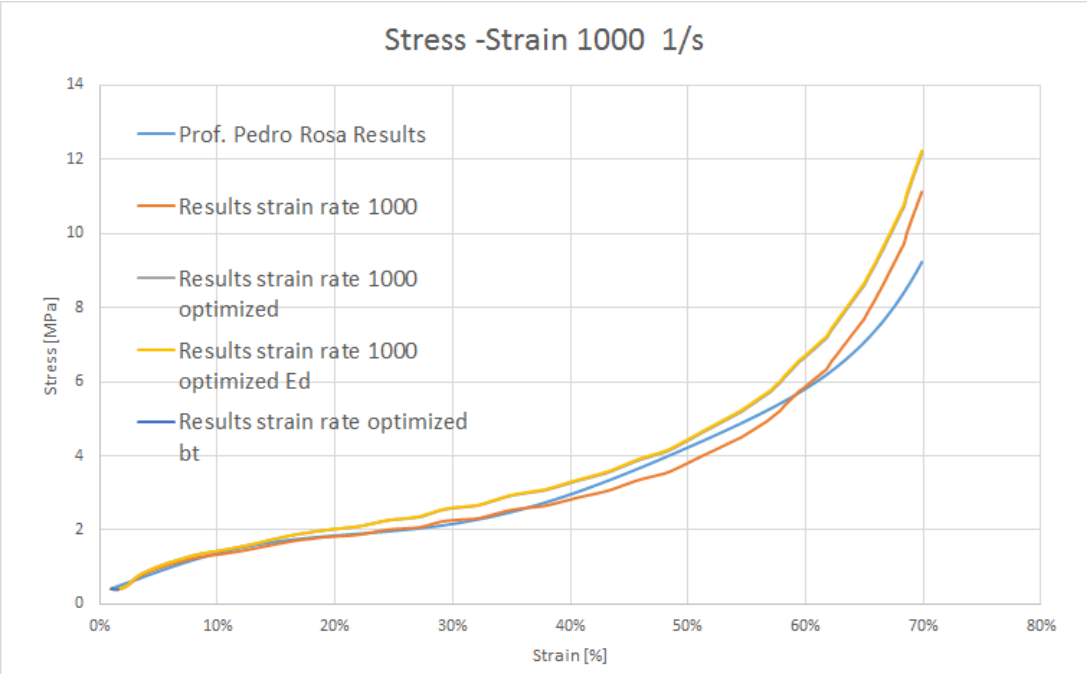

Figure 4.19: Strain Rate 1000 s^{-1} behaviour

Table 4.9: Tune for 1000 s^{-1}

Model	Raw model	Model Full opt.	Model with $E_d = 941409$ opt.	Model with $\beta_1 = 225.4$ opt.
Average error	-1%	-13%	-14%	-1%
Elastic error	-1%	-6%	-6%	-1%
Plateau Error	3%	-10%	-10%	3%
Densification error	-11%	-24%	-24%	-11%

For this strain rate (1000$s^{\cdot 1}$) everything that was said for the strain rate of 500 s^{-1} can be said again. The final conclusion about the strain rate optimization is that more work must be done in this area which becomes out of the scope of this thesis but in a general way the cork's behaviour in function of the strain rate in well represented by the initial model. In part this is true because cork is not much affected by the strain rate as can be seen the the following figure 4.20 derived from experimental testing and already confirmed by the reference [7].

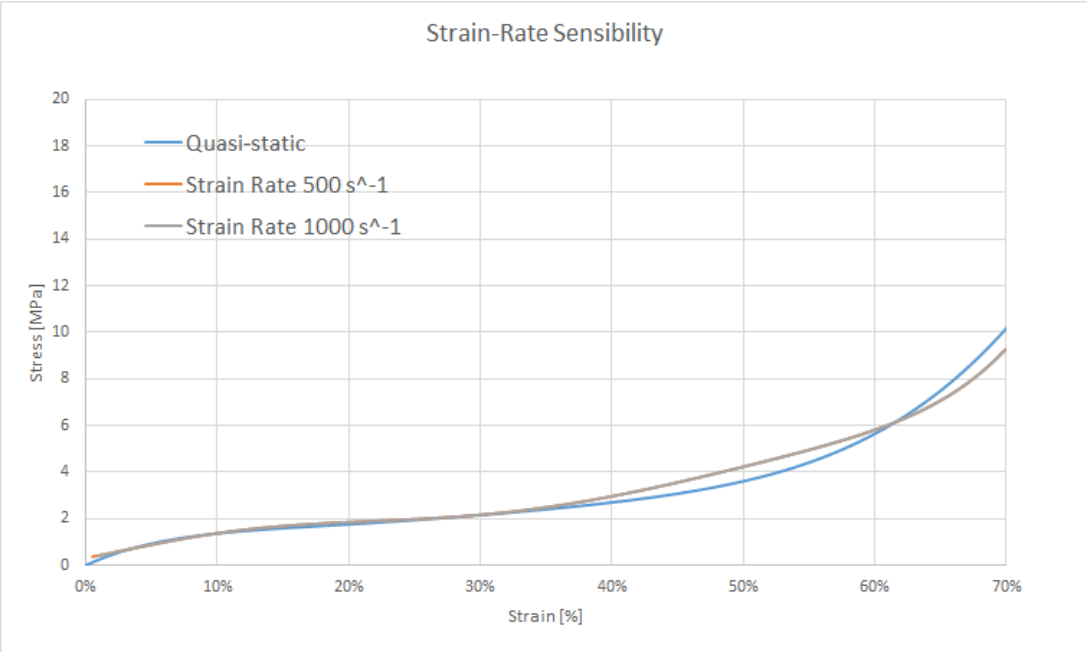

Figure 4.20: Strain Rate sensibility

4.5 Case Study 1 - 3 Point Bending

Now that the characterization of the cork was carried out it is time to put the model to the test. Since the test utilized for the characterization is a simple compression test one can try another fundamental test and take notice of the results and how well the Low density foam with solid formulation 1 can describe the behaviour of a cork specimen when subjected to 3 point bending. This test is based on the one presented in [35].

In this test a specimen with the measures indicated in the table 4.10 and in accordance with ASTM D790 was utilized.

Table 4.10: Specimen Data

Model	Dimensions [mm]
Depth	11
Width	44
Lenght	211.2
Support span	176

The setup utilized in this simulation is represented in the figure 4.21.

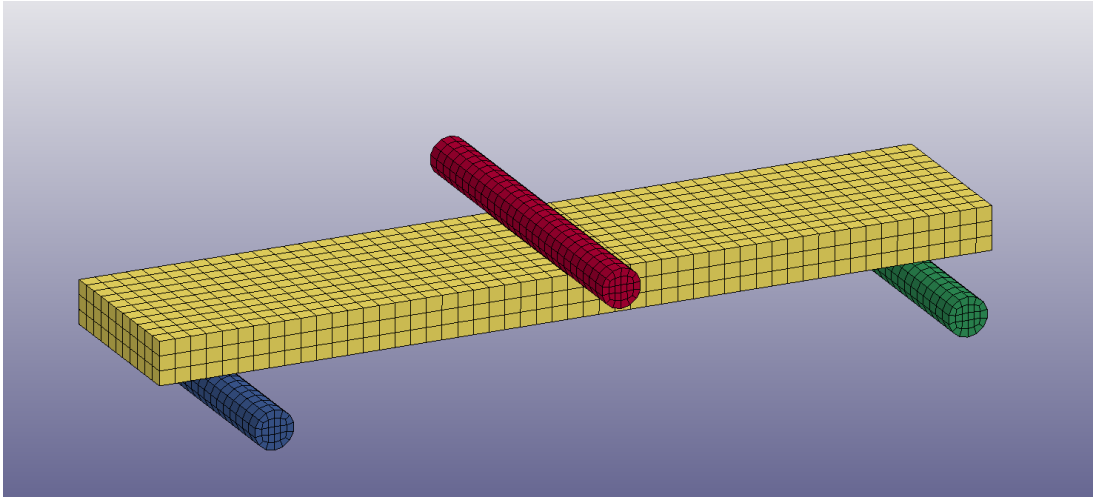

Figure 4.21: Setup

Of course care must be taken in order to maintain the same mesh parameters for which the inputs of the model were studied, in this case a mesh with about 4mm of edge is used. It may be expected that the results are not correct from the beginning, firstly because it is known that cork suffers from scale effects, this means that its mechanical behaviour and parameters are highly dependent on the size of the specimen in use. Secondly once the first test was in compression and in this model the behavior under uniaxial loading is not significantly coupled with the transverse ones, the Young modulus wasn't given much of importance since data for this value was also in lack.

The first results provided by the simulation are presented in the figure 4.22.

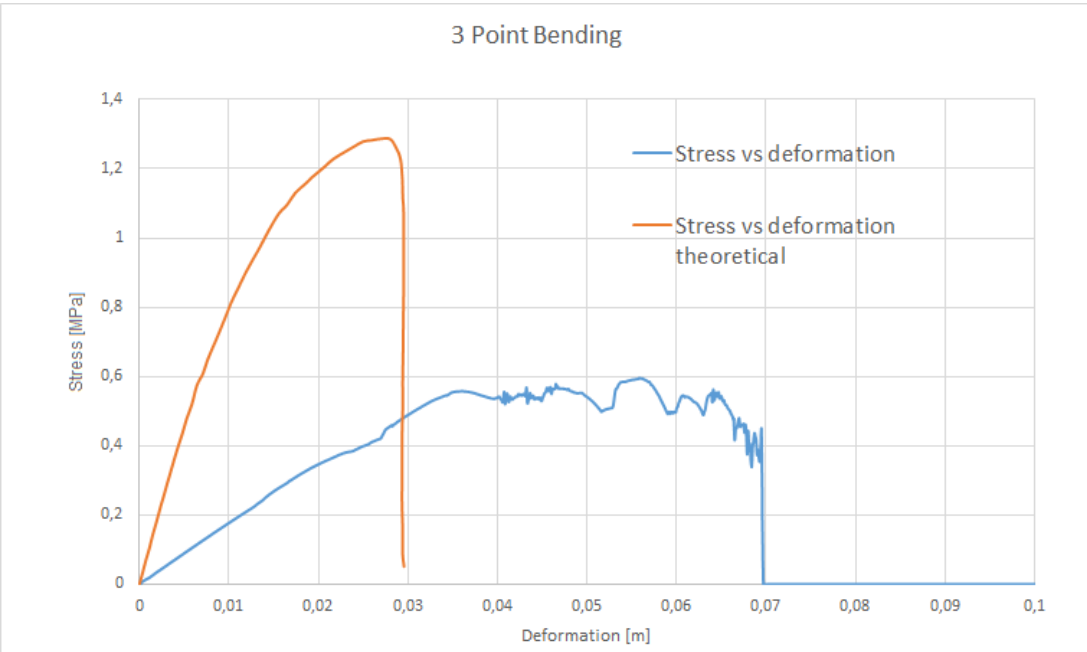

Figure 4.22: Bending Results

As can be seen the results from the simulations, the blue curve, has approximately the same shape as the experimental one represented in orange however the behaviour is not the same. There are

three main reasons why this can be happening. The first is the formulation used that can be good in compression but not for bending, the second problem is the scale factor, parameter that affect this kind of materials and represent the change in behaviour of a given specimen in function of its size and the third and most probable is the Young Modulus whose value was estimated due to the lack of information .

Testing first the formulation possibility and substituting solids 1 by solids -1. The results are presented in figure 4.23.

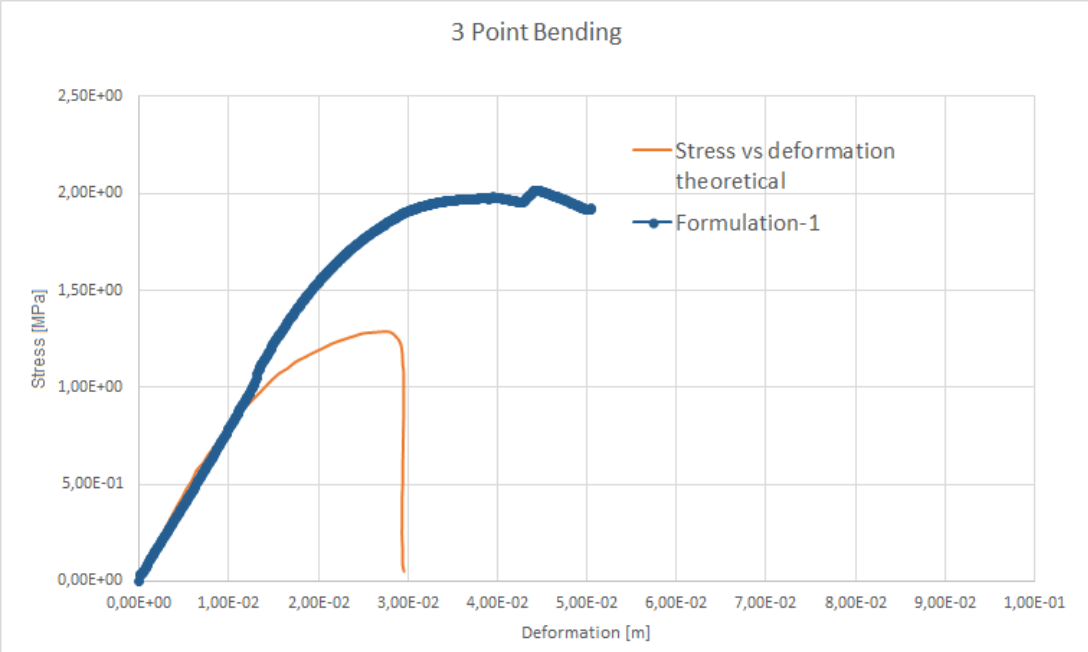

Figure 4.23: Bending results for formulation -1

The increase in integration point increased the rigidity of the specimen but this is not the solution still, the curve loses its shape at least in the spectrum of deformations intended.

The second solution is related to the scale factor of cork. It was found that indeed if a scale factor of 1/2.3 was applied to the stress vs deformation original curve 4.22 the behaviour takes a very close form to the experimental one represented in 4.24.

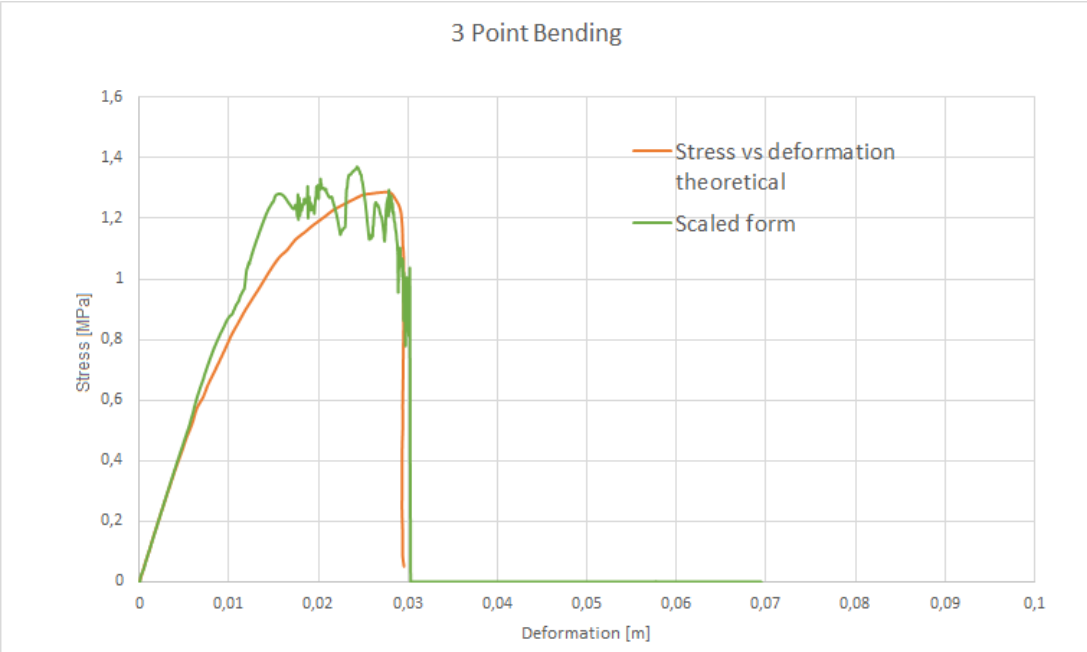

Figure 4.24: Bending results scaled

The value of 2.3 is consistence for example with the ratio of the width of the specimen in bending with the radius of the specimen in compression equal to 2.51. Of course this is a rough supposition and if by one side understanding the scale factor of cork gets out of the scope of this thesis for another side there is not enough data to make this conclusion.

Finally the last test and maybe the more acceptable one is to choose a Young's Modulus that satisfy the simulation curve needing more stiffness. The value attributed to the Young's Modulus is of 120 MPa and the results are presented in the figure 4.25.

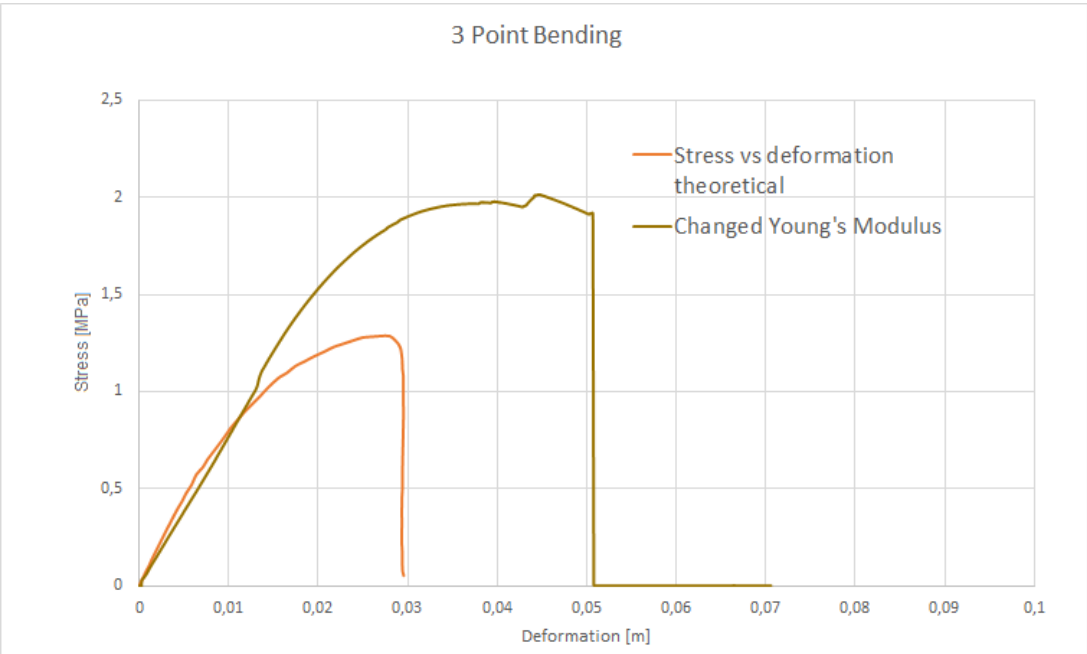

Figure 4.25: Bending results for changed Young Modulus

Non of the solutions presented above is the ideal one or even the correct one . It can be seen that the scaled curve is the best match to the hole curve but the one with improved Young modulus is the best solution having in mind that the use of scale factor is outside the scope of this thesis and even the LS-DYNA model has no way to represent it furthermore it gives more control over what is happening. The next figure 4.26 shows the Von Mises stresses in the specimen:

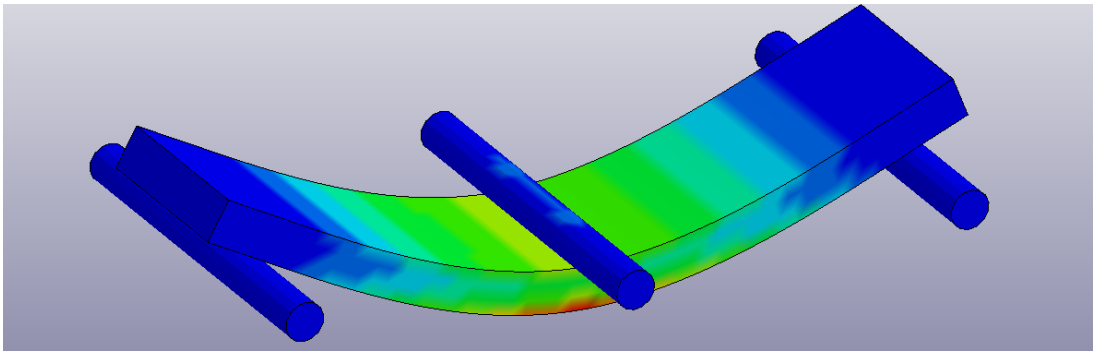

Figure 4.26: Von Mises bending results

4.6 Case Study 2 - Jet Engine Blade Containment

A containment test is a very important test in the aeronautical industry. In this context, containment test consist in a blade losing his support and being free while the rest of the fan is still rotating. The main objective of this test is to make sure that the blade does not leave the aluminium container so that no fragments leaves the engine at high speed and hit some part of the aeroplane putting it in a even more complicated situation.

For this simulation the used model, available in [36], consists on a simple aluminium container and two rotating blades where one of them loses it support. Moreover, to make sure the containment of the blade, a kevlar belt is incorporated along the aluminium container. The idea for this simulation begins with the offset of the kevlar belt in about 10 mm and incorporation of a layer of NL20 agglomerated cork in order to absorb energy from the impact, distribute it along the container and this way alleviate all the structure being even possible that no crack occurs as it is the case of the solo aluminium and kevlar belt. Figures 4.27 and 4.28 present above the deformations and Von Mises stresses for the model without cork and below the same but with cork respectively. In addition table 4.11 presents the summary of the solution.

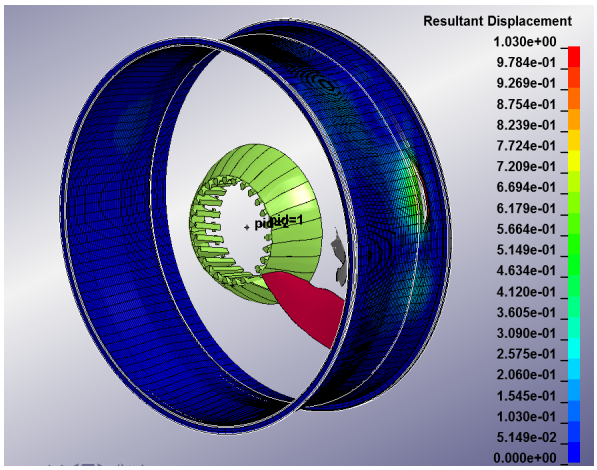

(a) Stress vs Strain

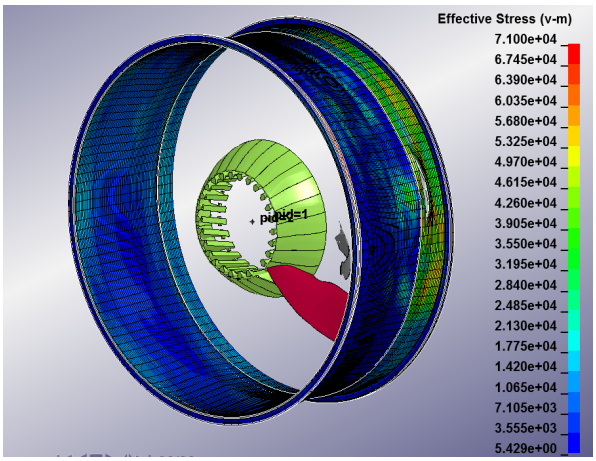

(b) Error vs Strain

Figure 4.27: Results without cork

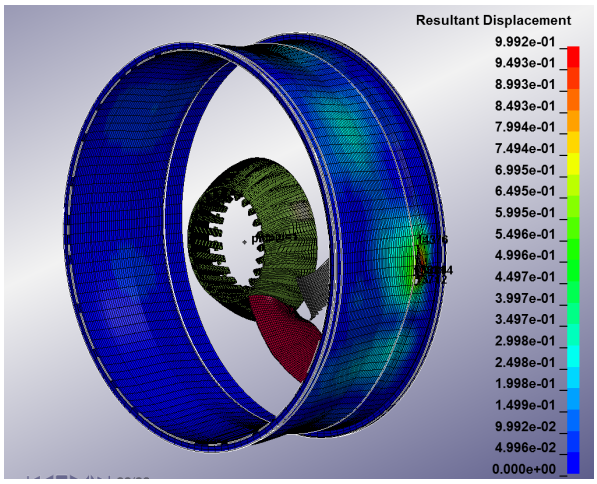

(a) Stress vs Strain

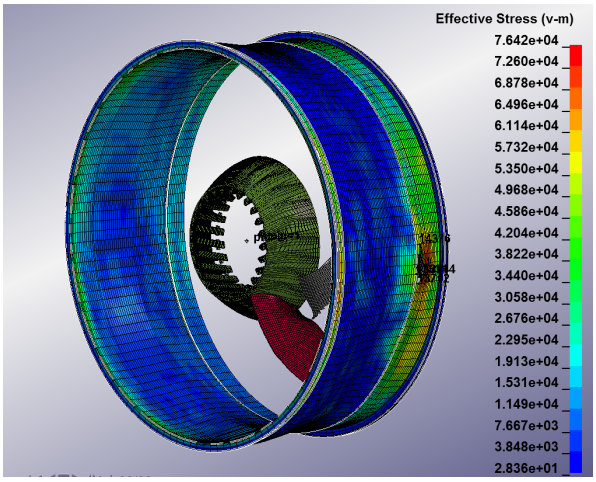

(b) Error vs Strain

Figure 4.28: Results with cork

The results obtained in the kevlar belt can be presented in the next table:

Table 4.11: Simulation Results

Kinetic Energy	Internal Energy	Max deformation	Max Von Mises	Cracks length	Cracks depth
Model without cork	4101.35J	26.16 mm	489.5 MPa	233.55mm	22.86mm
Model with cork	7784.65 J	25.15 mm	526.89 MPa	107.1mm	22.3mm
Gain	89.8%	-3.89%	7.1%	-54%	-2.5%

As can be seen there is an increase in the energy absorbed by the components around the cork, even though this was not expected, it makes sense. Cork in this case made possible the crack to be much more small and as consequence a big part of the energy was not releases by this mechanism, also it can be a lack of characterization on the cork energy dissipation parameters. What is left to a future user to understand is if the value added by the cork structure compensates the increase in the weight, in this specific case 1.59 Kg.

4.7 Case Study 3 - Ballistic Impact on sandwich panel

In this chapter a test was made on the utilization of cork as core of a sandwich panel with aluminium 2024 already validated by [36] as skins. The test was made first on a plate 4 mm thick then in a sandwich with two skins of 2 mm each and a core of 10 mm and 40 mm. The main objective was to notice the influence of cork in energy absorption from the bullet and definitely prove the efficiency or not of cork as core for ballistic applications. The bullet impact was also tested in 3 different velocities in order to understand if there is any spectrum of optimum performance to cork. Figure 4.29 presents the mesh and setup of this simulation. Beginning with the the plate impacted as 200 m/s the following figures 4.30 present a sequence of stages of the test.

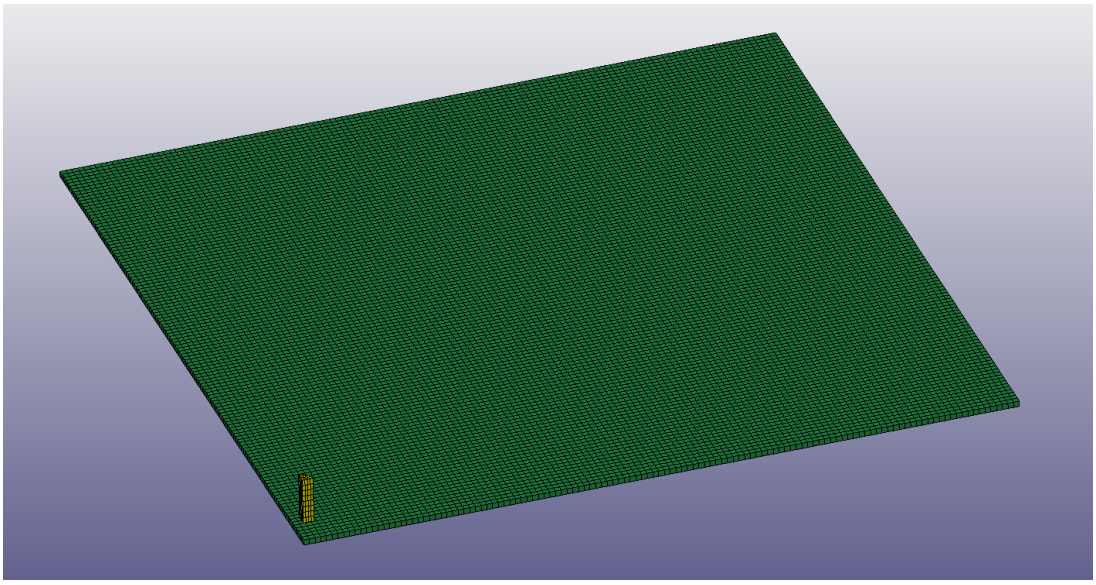

Figure 4.29: Mesh and setup to ballistic impact test (Plate Dimensions: 500mm x 500mm)

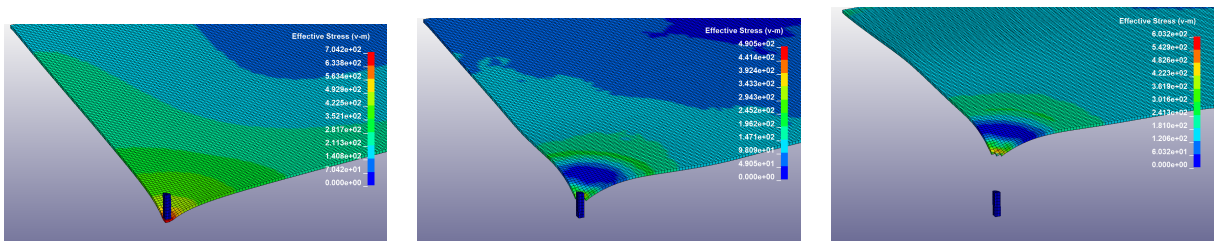

(a) Von Mises Stress -First Impact (b) Von Mises Stress- Penetration (c) Von Mises Stress- Outside the plate

Figure 4.30: Von Mises Stresses in Ballistic Impact

The Kinetic energy from the bullet in given in the table 4.12.

Table 4.12: Kinetic Energy Data

Kinetic Energy	200m/s
Initial K	224.47 J
Final K	224.47 J
Absorbed K	0%

The conclusions are that the plate alone as no influence on energy absorption from the bullet or that this absorption is so low that the software cannot notice this change. Moreover the shock wave propagated through all the plate which could have the consequences of propagating stress trough an entire vehicle. The next test used a layer of 10 mm made of cork. The mesh is in accordance with the converged model explained later. The results are presented in the next figures 4.31, 4.32, 4.33 the first row represent the impact for 200m/s the second raw 400m/s and the last row 1000 m/s.

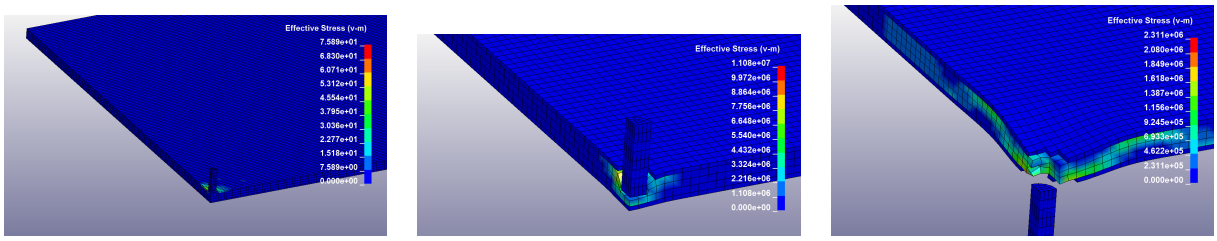

(a) Von Mises Stress-First Impact (b) Von Mises Stress-Penetration (c) Von Mises Stress-Leaving Plate

Figure 4.31: Ballistic Impact at 200m/s on 10mm core sandwich

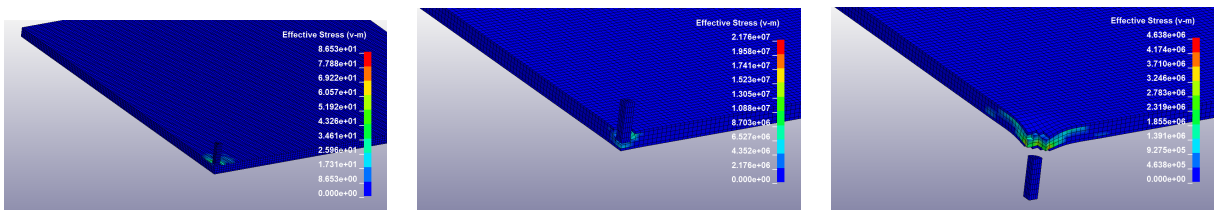

(a) Von Mises Stress-First Impact (b) von Mises Stress-Penetration (c) Von Mises Stress-Leaving Plate

Figure 4.32: Ballistic Impact at 400m/s on 10mm core sandwich

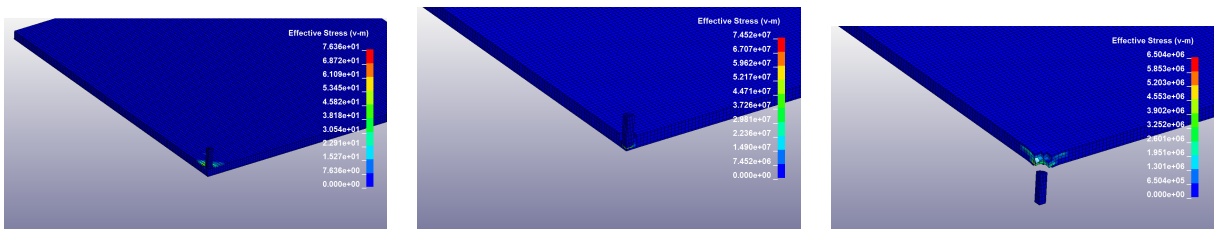

(a) Von Mises Stress-First Impact (b) Von Mises Stress-Penetration (c) Von Mises Stress-Leaving Plate

Figure 4.33: Ballistic Impact at 1000m/s on 10mm core sandwich

The results on the kinetic energy are presented in the following table 4.13.

Table 4.13: Kinetic Energy data for 10mm cork core

Kinetic Energy	200 m/s	400m/s	1000 m/s
Initial K	224.47	897.89J	5611.81 J
Final K	215.94 J	873.90 J	5522.31 J
Absorbed K	4%	3%	2%

From the results one can conclude that the cork did not added value to the absorption of energy, specifically in applications where weight is important. On the other hand, as can be seen for the pictures cork is much more useful in reducing the propagation of the shock waves.

Now it is useful to try to use a thicker layer of cork and understand how the variations in the thickness of cork influence the energy absorption capabilities. What is left to understand is if there is a significant gain in increasing the thickness. The results are presented in the next figures 4.34, 4.35 and 4.36. The first row represent the impact for 200m/s the second raw 400m/s and the last row 1000 m/s.

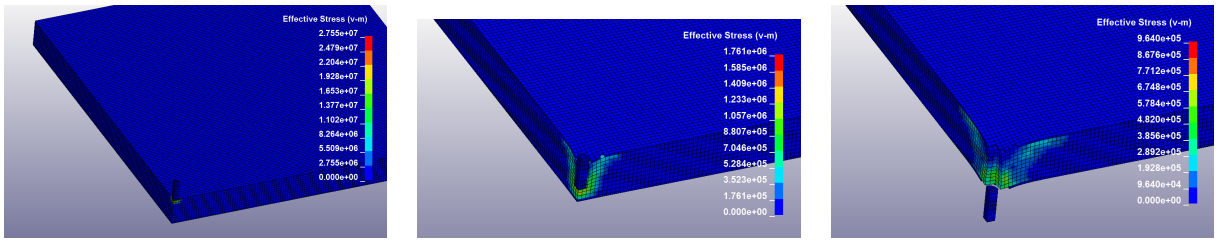

(a) Von Mises Stress- First Impact (b) Von Mises Stress- Penetration (c) Von Mises Stress- Leaving Plate

Figure 4.34: Ballistic Impact at 200 m /s on 40mm core sandwich

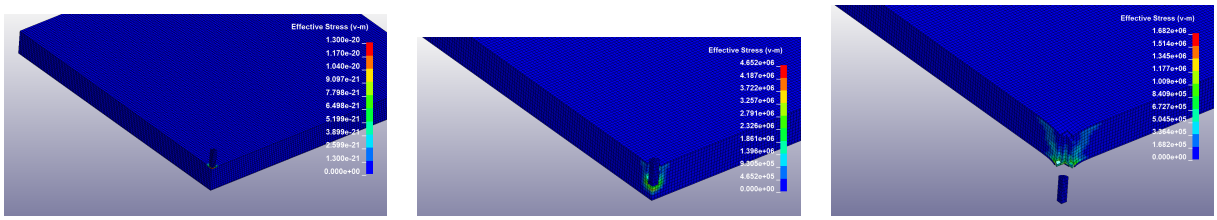

(a) Von Mises Stress- First Impact (b) Von Mises Stress- Penetration (c) Von Mises Stress- Leaving Plate

Figure 4.35: Ballistic Impact at 400 m /s on 40mm core sandwich

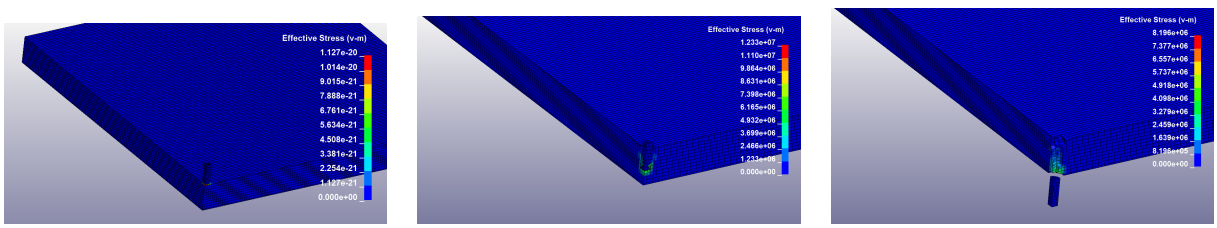

(a) Von Mises Stress- First Impact (b) Von Mises Stress- Penetration (c) Von Mises Stress- Leaving Plate

Figure 4.36: Ballistic Impact at 1000 m /s on 40mm core sandwich

The results on the kinetic energy are presented in the following table 4.14.

Table 4.14: Kinetic Energy data for 40mm cork core

Kinetic Energy	200 m/s	400m/s	1000 m/s
Initial K	224.47	897.89J	5611.81 J
Final K	195.61 J	806.16 J	5481.36 J
Absorbed K	13%	10%	2%

From the results one can conclude that there is an increase in the absorbed energy, this energy tend to become independent of the impact kinetic energy as was also concluded by [20]. Also with this results in figure 4.37 one can try to decide for a given application if and increase in weight compensates the increase in absorbed energy having in mind that for high impactor energies the thickness increase tends to have to effect on the absorbed energy.

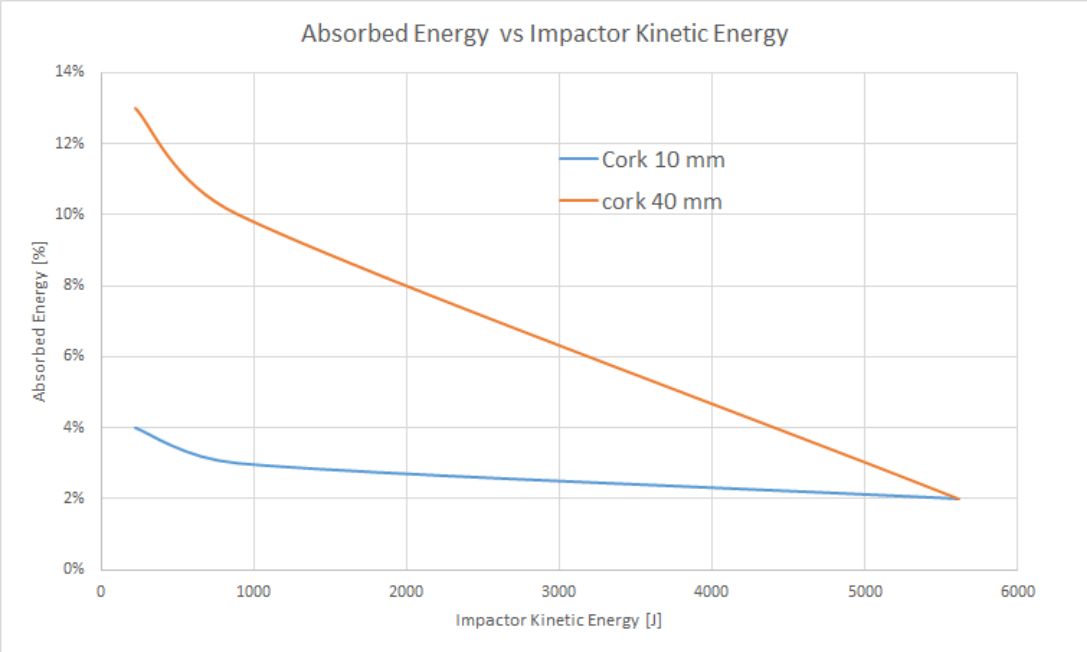

Figure 4.37: Absorbed Energy vs Impact K

Chapter 5

Conclusions and Future Work

In this chapter some general conclusions will be discussed and also the work that can be developed next using this thesis as basis .

5.1 Conclusions

Even though some conclusions specific for each simulation were taken as the thesis is presented there are still some general conclusions to be taken that are related to the use of cork.
In the actual circumstances the best way to characterize the compressive behaviour is the Low Density Foam however everything indicates that due to the variety of parameters that can be used, honeycomb model may have the degrees of freedom needed to describe with precision all the regions of the cork compression behaviour, its sensibility to strain rate and even tension tests, bending and so on.
With the model chosen, it can be verified that there is an high dependence of the results on the mesh but from a certain number of elements the error tends to stabilize , this value of stabilization is not the most important because what is really important is to keep the errors as low as possible in all the regions of the stress-strain curve and still maintain the processing time in a acceptable value. Moreover is important to realize that cork as a natural material has a high variance in characteristics, this means that the errors obtained when comparing the computational results with experimental one can be much different if the experimental specimen is changed. This was the reason why the Formulation 1 with 24 elements was chose, it keeps the processing time low at the same time that the errors and average errors are low.
Going on to the bending case study is is verified that there is no data available to have a good characterization of cork in this kind of test. This is the main reason why it is advisable to use this material model in components were the main forces actuating are compressive ones. Still in this test the value 1/2.51 found as scale factor for the bending behaviour curve may be related to the scale factor of the material but that cannot be concluded by the simulations done.
The test on the jet engine containment test demonstrated that cork was not good in absorbing energy, the quantities of kinetic energy are huge and as seen in the previous section cork loses his capacity to absorb energy as the kinetic energy increases. On the other hand the crack caused by the blade is

much more small and since this is a containment test the objective is achieved with more efficiency.
Finally the test on ballistic impact allowed to conclude that cork may in fact be a good choice as long as the impact energy in kept low enough. For cases where the energy of the impactor is hight the quantity of absorbed energy is very low and even the thickness of the core loses his importance. One area where this kind is really capable of being excellent is the transmition of vibration and shock waves, even though this test was not specifically made, it can be seen for the figures that when compared to the plate alone the impact damage is much more localized and the stress wave is much more contained in a given area which can be an excellent characteristic in some cases.
Summarizing one can say that cork may have is field of application in components where vibration absorption is a must and/or the impactor energy has low Kinetic Energy. This characteristics associated with the fact of being a cheap and renewable material make of this material a very appellative one in the current days.

5.2 Future Work

As future work one can enumerate by order of importance the tasks needed to present a full model of cork:

1. Experimental Testing in tension, bending and shear at different strain rates;
2. Study and experimental testing on the failure mechanisms of cork;
3. Re-iteration of the Low Density Foam model presented in this thesis;
4. Testing the inputs obtained in 1 and 2 on the Honeycomb material model and compare the results with the ones from Low Density Foam;
5. In case of integration of this material in the industry it is necessary to to reduce the variability of this natural material. The only solution to make this control is to improve the production methods.

Also it can be said that cork has such a *sui generis* behaviour that the only effective way to tackle this problem is to develop from scratch a new material model, compile it and integrate it in LS-DYNA.

Bibliography

[1] C. Technologies. Cellular materials, 2015. URL www.cellmattechnologies.com/en/home/cellular-materials/. Acessed on 05/09/2016.

[2] L. J. Gibson. Biomechanics of cellular solids. *Journal of Biomechanics*, 38:377–399, 2005. doi: 10.1016/j.jbiomech.2004.09.027.

[3] S. P. Silva, M. A. Sabino, E. M. Fernandes, V. M. Correlo, L. F. Boesel, and R. L. Reis. Cork : properties , capabilities and applications. *International Materials Reviews*, 50(6):345–366, 2005. doi: 10.1179/174328005X41168.

[4] J. Lopes, R. Moreira, and J. Rodriques. Experimental identification of dynamic properties of cork compound. In *5th International Conference on Mechanics and Materials in Design*, 2006.

[5] F. Teixeira Dias, V. Miranda, C. Gameiro, J. Pinho-da Cruz, and J. Cirne. Impact behaviour of aluminium foam and cork in energy absorbing systems. In *2nd WSEAS Int. Conference on Applied and Theoretical Mechanics*, pages 148–153, 2006.

[6] J. F. Mano. Creep-recovery behaviour of cork. *Elsevier Material Letters*, 61:2473–2477, 2007. doi: 10.1016/j.matlet.2006.03.157.

[7] C. P. Gameiro and J. Cirne. Dynamic axial crushing of short to long circular aluminium tubes with agglomerate cork filler. *International Journal of Mechanical Sciences*, 49:1029–1037, 2007. doi: 10.1016/j.ijmecsci.2007.01.004.

[8] P. Carvalho. Análise do comportamento mecânico e identificação do tipo de falha em estruturas sandwich com núcleos de cortiça. Master's thesis, Instituto Superior Técnico, 2008.

[9] M. Santos. Aplicação Estrutural de Cortiça para Melhoria da Segurança Passiva em Caso de Impacto. Master's thesis, Universidade de Aveiro, 2008.

[10] P. J. Antunes. *Constitutive Modelling of Cork-Polyurethane Gel Composites*. PhD thesis, Universidade do Minho, 2008.

[11] J. Lopes. Modeling the Dynamic Behavior of Laminate Structures with Cork Compounds. Master's thesis, Faculdade de Engenharia da Universidade do Porto, 2008.

[12] L. Paulo. A Preliminary Study on Passive and Active Flutter Suppression Concepts for Aeronautical Components Acknowledgments. Master's thesis, Universidade da Beira Interior, 2009.

[13] N. Franco. Caracterização mecânica de um material híbrido de Carbono / Epoxy e Cortiça. Master's thesis, Universidade da Beira Interior, 2009.

[14] C. Nunes. Impacto de Baixa Velocidade em Estruturas Sandwich à Base de Cortiça Agradecimentos. Master's thesis, Universidade da Beira Interior, 2009.

[15] O. Castro, J. Silva, T. Devezas, A. Silva, and L. Gil. Cork Agglomerates as an Ideal Core Material in Lightweight Structures. *Journal of Materials and Design*, (May), 2009. doi: 10.1016/j.matdes.2009.05.039.

[16] L. Reis and A. Silva. Mechanical Behavior of Sandwich Agglomerates as Core Materials. *Journal of Sandwich Structures and Materials*, 2009. doi: 10.1177/1099636209104523.

[17] L. Bom. Comportamento à compressão e tracção da cortiça : estudo numérico. Master's thesis, Universidade de Aveiro, 2010.

[18] R. Coelho. Development of protection systems using cellular materials. Master's thesis, Universidade de Aveiro, 2010.

[19] M. Píriz. Passive vibration control of aerospace structures based on viscoelastic materials. Master's thesis, Universidade da Beira Interior, 2011.

[20] S. Sanchez-saez, E. Barbero, and J. Cirne. Experimental study of agglomerated-cork- cored structures subjected to ballistic impacts. *Materials Letters*, 65(14):2152–2154, 2011. doi: 10.1016/j.matlet.2011.04.083.

[21] J. d. S. Martins. *Blast-wave absorption capacity of sandwich structures incorporating cellular materials*. PhD thesis, Universidade de Aveiro, 2012.

[22] R. Fernandes. Caracterização à Fractura de um Material Compósito com Carbono-Epóxido e Cortiça. Master's thesis, Faculdade de Engenharia da Universidade do Porto, 2013.

[23] J. Lopes. Effects of Design Parameters on Damping of Composite Materials for Aeronautical Applications. Master's thesis, Universidade da Beira Interior, 2013.

[24] G. Serra. Resposta ao Impacto de Painéis Sanduíche. Master's thesis, Universidede da Beira Interior, 2013.

[25] M. Costas, J. Diaz, S. Hernandez, and A. Tielas. Static and dynamic axial crushing analysis of car frontal impact hybrid absorbers. *International Journal of Impact Engineering*, pages 166–181, 2013. doi: 10.1016/j.ijimpeng.2013.06.011.

[26] H. Policarpo. *Numerical and experimental models for vibration attenuation using cork composite materials*. PhD thesis, Technical University of Lisbon, 2013.

[27] T. Castilho. Impact Resistance of Marine Sandwich Structures . Master's thesis, Instituto Superior Técnico, 2014.

[28] F. A. O. Fernandes, R. Pascoal, and R. Alves de Sousa. Modelling impact response of agglomerated cork. *Materials and Design*, 58:499–507, 2014. doi: 10.1016/j.matdes.2014.02.011.

[29] S. Sanchez-saez, E. Barbero, S. K. Garcia-castillo, I. Ivañez, and J. Cirne. Experimental response of agglomerated cork under multi-impact loads. *Materials Letters*, 160:327–330, 2015. ISSN 0167-577X. doi: 10.1016/j.matlet.2015.08.012. URL `http://dx.doi.org/10.1016/j.matlet.2015.08.012`.

[30] Y. Sue Chua, E. Law, S. D. Pang, and S. T. Quek. Fish scale-cellular composite system for protection against low-velocity impact. *Composite Structures*, 145:217–225, 2016. ISSN 0263-8223. doi: 10.1016/j.compstruct.2016.02.070. URL `http://dx.doi.org/10.1016/j.compstruct.2016.02.070`.

[31] L. Gibson. Cellular solids: Structure, properties and applications, 2014. URL `ocw.mit.edu/courses/materials-science-and-engineering/3-054-cellular-solids-structure-properties-and-applications-spring-2014/index.htm`. Acessed on 07/08/2016.

[32] LS-DYNA. Ls-dyna keyword user's manual volime ii-material models, 2014. URL `www.lstc.com/download/manuals`. Acessed on 12/08/2016.

[33] S. Strenght of materials-lecture 12, 2009. URL `nptel.ac.in/courses/112107146/12#`. Acessed on 12/08/2016.

[34] A. C. Composites. Corecork by amorim, 2009. URL `http://www.matrix-composites.co.uk/prod-data-sheet/cork/mds-gama-corecork.pdf`. Acessed on 22/07/2016.

[35] L. Reis, B. Soares, and L. Sousa. Cork composites and their role in sustainable development. *Engineering Procedia*, 2011.

[36] L.-D. A. W. Group. Aluminium 2024, 2013. URL `awg.lstc.com`. Acessed on 12/09/2016.

[37] *Cork: Biology, Production and Uses*. Elsevier Science, 2007.

[38] N. Lakreb, B. Bezzazi, and H. Pereira. Mechanical behavior of multilayered sandwich panels of wood veneer and a core of cork agglomerates. *Materials & Design*, 65:627–636, jan 2015. ISSN 02613069. doi: 10.1016/j.matdes.2014.09.059. URL `http://www.sciencedirect.com/science/article/pii/S0261306914007614`.

[39] naldzgraphics. 30 sets of free cork texture, 2016. URL `naldzgraphics.net/textures/free-cork-texture/`. Acessed on 07/09/2016.

[40] P. A. of Cork. What is it?, 2016. URL `www.apcor.pt/en/cork/what-is-it/`. Acessed on 07/09/2016.

[41] P. A. of Cork. Cork harvesting, 2016. URL www.apcor.pt/en/cork/processing/cork-harvesting/. Acessed on 07/09/2016.

[42] R. J. Barros and Pereira. Análise estrutural de vigas sandwich de alumínio-aglomerado de cortiça. 2014.

[43] LS-DYNA. Ls-dyna theory manual, 2016. URL www.lstc.com/download/manuals. Acessed on 12/08/2016.

[44] T. Erhart. Review of solid elements formulations in ls-dyna- properties, limits, advantages and disadvantages, 2011. URL www.dynamore.de/de/download/papers/forum11/entwicklerforum-2011/erhart.pdf. Acessed on 12/08/2016.

[45] *LS-DYNA User's Manual*. LS-DYNA, 2015.

Appendix A

Cork

A.0.1 Cork

Cork is a natural cellular material with properties that make it a very good alternative to synthetic sandwich cores. It has an alveolar structure similar to honeycomb but with closed cells, low density and excellent insulation properties. Also it is a renewable raw material from a sustainable source. The composition corks or agglomerates are made with cork granules of variable dimensions that are gethered together using an adhesives (e.g. polyurethane, melamine etc). Although the composition cork agglomerates retain most of the properties of the cork as natural material as summarized in [37], the mechanical strength of a specific composite cork product is also related to the properties of the adhesive [38].The figure A.1 shows an example of cork.

Figure A.1: Cork (Source [39]).

Systematizing the propreties of cork the following can be enumerated from the source [40]:

1. Lightweight;
2. Waterproof;
3. Gasproof;
4. Elastic and compressible
5. Excelent thermal insulator;

6. Excelent acoustical isolator;
7. Slow burning;
8. Antistatic;
9. Anti-allergic;
10. Wear resistane.

As can be seen by the propreties above, cork can be used for many purposes once it is a very polivalent material. This puts Portugal in a very advantageous position once it is in the front line of cork production and exportation. As to the life cycle of the tree it is very simple but long, it takes 25 years for a cork oak tree to produce an usable and profitable cork. The harvesting takes place between the months of May and August only if the tree circumference reach 70 cm when measured 1.3m above the ground level. From that moment on the tree can be harvested by an average of 150 years. The first time a tree is harvested is called ”desbóia” and produces a cork that is a very irregular one (virgin cork) used for applications other than cork stoppers. Nine years later the second harvest produces material much more regular called secondary cork that is not suitable for cork stoppers still. It is from the third harvest that the cork with the best properties is obtained, called ”amadia” or reproduction cork. From then on the cork oak will supply good cork for every nine years [41]. In Figure A.2 is presented the 6 phases of harvesting cork.

Figure A.2: Phases of cork harvesting (Source [41]).

Cork Morphology

Understanding the morphology of cork is essential in order to understand some of its mechanical properties. In 1664 Robert Hooke verified the cellular structure of cork (figure A.3) understanding its anisotropy based on the fact that two perpendicular sections were not equal.

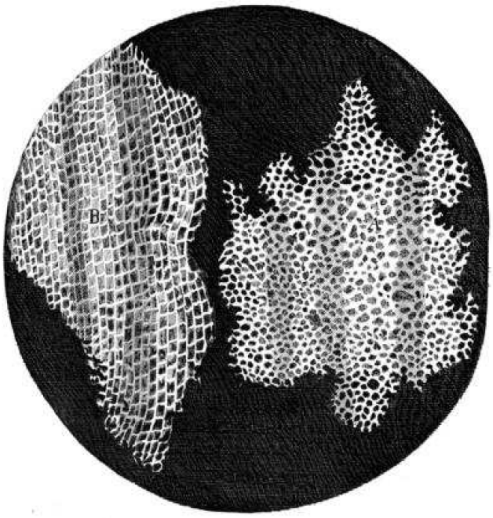

Figure A.3: Hooke's cork observation(Source [31])

From the observations it was clear that in fact there were 3 main directions identifiable:

1. Radial - Direction of the trunk radius;
2. Axial - Direction of the tree trunk;
3. Tangential - Direction of the circumference of the trunk.

The figure A.4 shows the main directions in the cork.

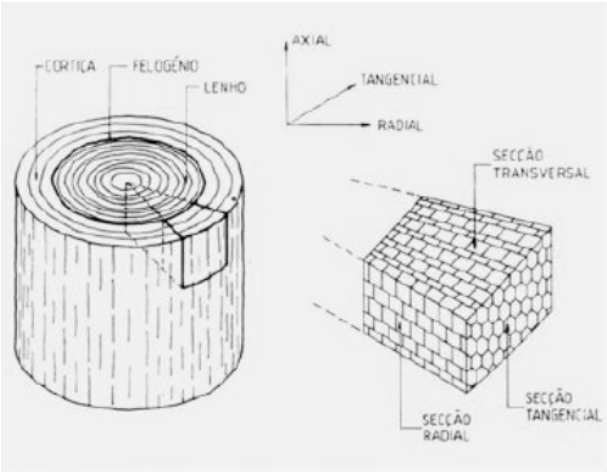

Figure A.4: Cork main directions (Source [17])

The cells are hexagons cells stacked in columns in which its axis is radial to the tree trunk. This direction is usually corrugated as seen in the figure A.5.

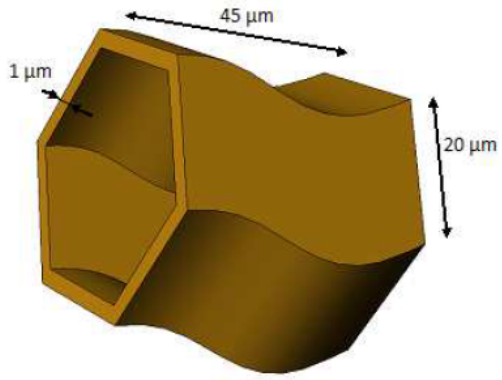

Figure A.5: Cork Cell (Source [9])

One last indication to make is that once the cells are open at the surface the coefficient of friction can assume very high values.

Cork Mechanical Properties

The cork presents very particular mechanical characteristics. This can be clearly viewed in a plot of compression behaviour. This happens because this kind of cellular material behaves as a viscoelastic material. The figure A.6a) present the compression behaviour of cork and the second represents its behaviour in tension A.6 b).

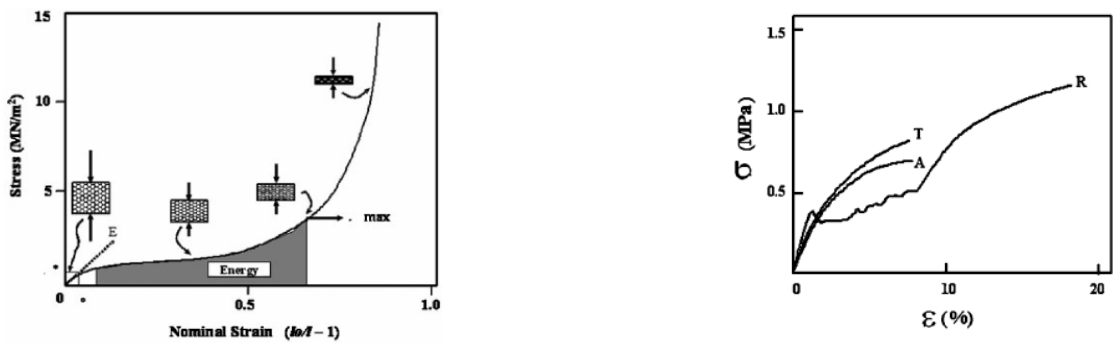

(a) Cork Behaviour in Compression

(b) Cork Behaviour in Tension

Figure A.6: Cork mechanical behaviour (Source [42])

As can be seen in the compression figure there is a first zone to 7% extension where the cells walls are subjected to elastic flexure. After 7% and before 70% the region is almost horizonal and is cause by the buckling of the cells walls. After 70% the walls are completely colapsed and smashed giving origin to a hardening of the material. One important characteristic to have in mind is that if the compression

is in the radial direction there will be a small dilatation in non radial direction giving rise to a positive Poisson Coeficient. If the compression is on a non radial direction the Poisson Coeficient is negative [42]. For the tension figure it can be seen that the tangential-T and Axial-A direction differ a lot from the radial-R direction. This happens because while in the tangential and axial direction the cells fracture at the limit tension of the material, on the radial direction cells will sequentially fail giving origin to the wavy behaviour . One last point to have in mind is that the Young Modulus of the material in compression is substancial inferior to the Young Modulus of the Material in tension. This happens because the cells become more rigid as the curvature amplitude of the walls become inferior [42].

As to the behaviour of the cork agglomerates, they can vary substantially because they are mixes of many kinds of cork, with resins and sometimes with rubbers and other components.

Appendix B

Finite Element Method-LS-DYNA

B.0.1 Finite Element Method

The fundamentals of finite element formulation is not the aim of this thesis, however the understanding of how LS-DYNA deals with a determined problem can be interesting . Consider for example the following body and notation in the figure B.1:

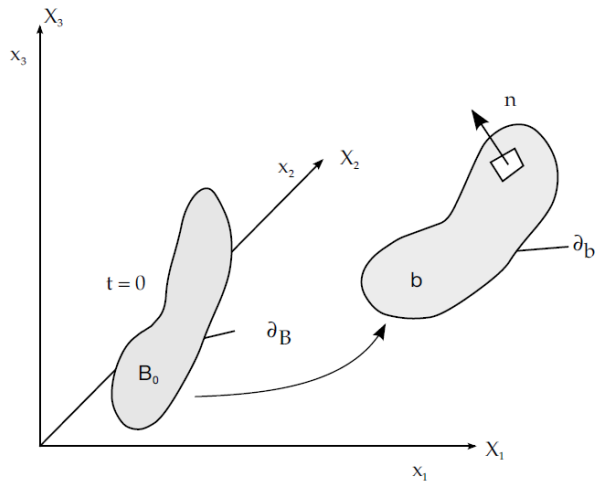

Figure B.1: Body and Notation (Source [43]).

The objective is to seek for a time-dependent deformation in which a point in B initially at x_0 in a rectangular Cartesian coordinate system moves to x_i. For this and adopting a Lagrangian formulation on can assume B.1:

$$x_i = x_i(x_0, \tau) \tag{B.1}$$

And subjected to the initial conditions B.2 and B.3:

$$x_i(x_0, 0) = X_i \tag{B.2}$$

$$\dot{x_i}(x_0, 0) = v_i(\chi) \tag{B.3}$$

Where v_i is the initial velocity.

Governing Equations

The main objective must be within a certain limit that defines the physical world. To make sure that this happens some equations must be satisfied:

1. Momentum Equation B.4:

$$\sigma_{ij,j} + \rho f_i = \rho \ddot{x}_i \tag{B.4}$$

   Where ρ is the density of the body, f_i are the body forces and σ is the stress.

2. Mass Conservation B.5

$$\rho V_r = \rho_0 \tag{B.5}$$

   Where this V_r is the relative volume.

3. Energy equation B.6

$$\dot{Energy} = V s_{ij} \dot{\epsilon_{ij}} - (p+q)\dot{V} \tag{B.6}$$

Where s_{ij}, p, q,δ_{ij} and $\dot{\epsilon}_{ij}$ represent the deviatoric stress, pressure, bulk viscosity, Kronecker delta and the strain rate tensor respectively. The above equation is integrated in time and used for evaluate and track global energy balance. Gathering all the equations one can get the weak form of the equilibrium equation which is a statement of the principle of virtual work B.7:

$$\delta\pi = \int_v \rho \ddot{x}_i \delta x_i dV + \int_v \sigma_{ij} \delta x_{i,j} dV - \int_v \rho f_i \delta x_i dV - \int_{\partial b1} \varpi \delta x_i dS = 0 \tag{B.7}$$

Where ϖ is the traction tensor. The imposed mesh permits that each node is tracked through time thanks to B.8:

$$x_t(x_0, \tau) = x_i(x_0)(\xi, \eta, \zeta), \tau) = \sum_{j=1}^{k} N_j(\xi, \eta, \zeta) x_i^{nodal}(\tau) \tag{B.8}$$

where N_j are the shape or interpolation functions in the parametric coordinates ξ, η, ζ, k is the number of nodes, x_i^{nodal} is the nodal coordinate of the jth node in the ith direction.
Knowing that $\delta\pi = \sum_{m=1}^{n} \delta\pi_m = 0$ holds for each element, taking all contributions in account and using the approximation from equation B.8 the final form becomes B.9:

$$\sum_{m=1}^{n} \{ \int_{v_m} \rho N_m^T N_m a dV + \int_{v_m} B_m^T \sigma dV - \int_{v_m} \rho N_m^T f dV - \int_{\partial b_1} N_m^T \varpi dS \} = 0 \tag{B.9}$$

Where N is an interpolation matrix, σ is the stress vector, B is the strain-displacement matrix, a is the nodal acceleration vector, f is the body force load vector and ϖ is the applied traction load.

Time Integration

As said before there is the need to study the body behaviour in time. To do that there is a necessity to integrate time in the equations using some numerical method. This method is called Central Finite

Difference Method. Consider the equation of motion B.10:

$$[M]a^n = [P]^n - [F]^n + [H]^n \tag{B.10}$$

Where M is the diagonal mass matrix, P^n accounts for all internal and body forces, F^n is the stress divergence vector and H^n is the hourglass resistance effect that will be explained later in this appendix. To advance to τ^{n+1} the central difference method is utilized for acceleration B.11, velocity B.12 and position B.13:

$$a^n = M^{-1}([P]^n - [F]^n + [H]^n) \tag{B.11}$$

$$v^{n+1/2} = v^{n-1/2} + a^n \Delta\tau^n \tag{B.12}$$

$$d^{n+1} = d^n + v^{n+1/2}\Delta\tau^{n+1/2} \tag{B.13}$$

where $\Delta\tau^{n+1/2}$ is given by equation B.14 and x^{n+1} by equation B.15 :

$$\Delta\tau^{n+1/2} = \frac{\Delta\tau^n + \Delta\tau^{n+1}}{2} \tag{B.14}$$

$$x^{n+1} = x_0 + d^{n+1} \tag{B.15}$$

Solid Elements

The equations that rule the formulations for solid element is extensive and there is no added value to the thesis in the deduction of the equations. What is necessary to know is that the formulations used for this thesis and shown in figures B.2, B.3, B.4, B.5, B.6 have impact in the N matrix explained in the previous subsection. Without entering in many details it is important to know what are the capabilities and limitation of each element used in this thesis:

- Formulation 1:

  1. Underintegrated constant stress;
  2. Efficient and accurate;
  3. Works for severe deformations;
  4. Needs hourglass stabilization

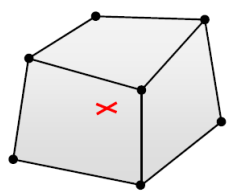

Figure B.2: Form. 1 (Source [44])

- Formulation 2:

1. Selective reduced integrate brick element - Volume locking alleviated;
2. Too stiff in many situations especially for poor aspect ratios (shear locking);
3. Slower than formulation 1;
4. No needs for hourglass stabilization
5. More unstable for large deformations

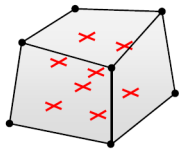

Figure B.3: Form. 2 (Source [44])

- Formulation -1:

1. Similar to type 2 but accounts for poor aspect ratio in order to reduce shear locking;
2. Efficient Formulation;
3. Hourglass tendencies

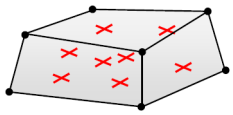

Figure B.4: Form. -1 (Source [44])

- Formulation -2:

1. Similar to type 2 but accounts for poor aspect ratio in order to reduce shear locking;
2. Accurate Formulation;
3. Higher Computational costs than -1 formulation

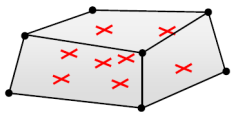

Figure B.5: Form. -2 (Source [44])

- Formulation 3:

1. Quadratic 8 node hexahedron with 6 dof per node
2. Derived from 20 node hexahedron;
3. Full integration 12 points;
4. Applicable for connections with shells;
5. Good accuracy for small strains;
6. Tendency to volumetric locking.

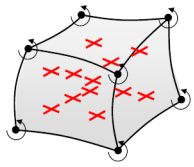

Figure B.6: Form.3 (Source [44])

Hourglass

Although one point integration is faster, there is a big disadvantage in using it which is the necessity of controlling the zero energy modes also called hourglass modes represented in B.7:

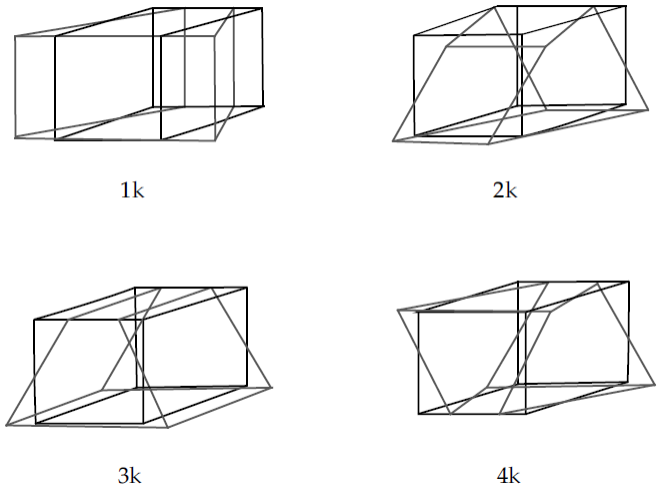

Figure B.7: Hourglass modes (Source [43])

In a numerical simulation there is the need to keep this values low by controlling it and imposing some type of correction. There are many ways to do that and the study of these parameter doesn't concern this thesis. What concerns this work is to keep hourglass below values. More information about hourglass may be studied in [43].

Time step

When solving the equations LS-DYNA loops through the elements to update the stresses and the right hand side force vector. Also a new time step size is determined by taking the minimum value between all elements. This parameter is very important because it depends on the mesh and makes then simulation

heavier and slower. This step time is given by equation B.16:

$$\Delta\tau_e = \frac{L_e}{(Q + (Q^2 + c^2)^{1/2})'} \tag{B.16}$$

Where Q is a funtion of the bulk viscosity, L_e is a characteristic length given by the ratio of the volume of the solid element by the biggest area of the element's faces and c is the adiabatic sound velocity.

B.0.2 Optimization Technique

The last topic on the modelling of cork's behaviour is the fine tuning of the model to adapt the unknowns parameters of the material to the experimental data available. In this particular case the unique behaviour that is intended to improve is the parameter that deals with rate effects. For this a Metamodel-based optimization was chosen with a sequential domain reduction strategy. In this strategy the sampling is done sequentially and smaller number of points is chose for each iteration. This approach has the advantage that the iterative process can be stopped as soon as the metamodels or optimum points have achieved sufficient accuracy accelerating the process. The fundamental idea behind is an adaptive domain reduction strategy to reduce the size of the region. During a particular iteration the new points are inserted within a subregion of the design space. This strategy is useful for a kind of optimization in which the unique interesting result is the final optimal point and not any global exploration of the design. For details on the optimization theory one can consult [45].